Cell-to-cell heterogeneity in Sox2 and Brachyury expression guides progenitor destiny by controlling their movements.

Michèle Romanos [1,2,*] ; Guillaume Allio [1,*]; Léa Combres [1]; Francois Médevielle [1] ; Nathalie Escalas [1]; Cathy Soula[1], Ben Steventon [3]; Ariane Trescases [2], Bertrand Bénazéraf [1, #]

Affiliations :

[1]Centre de Biologie du Développement (CBD), Centre de Biologie Intégrative (CBI), Université de Toulouse, CNRS, UPS, Toulouse, France.

[2]Institut de Mathématiques de Toulouse UMR 5219, Université de Toulouse, CNRS, 31062 Toulouse Cedex 9.

[3]Department of Genetics, University of Cambridge, Cambridge CB2 3EH, UK

* Co-first authors

Corresponding author: bertrand.benazeraf@univ-tlse3.fr

Abstract :

Although cell-to-cell heterogeneity in gene and protein expression has been widely documented within a given cell population, little is known about its potential biological functions. We addressed this issue by studying posterior progenitors, an embryonic cell population that is central to vertebrate posterior axis formation. These progenitors are able to maintain themselves within the posterior region of the embryo or to exit this region to participate in the formation of neural tube or paraxial mesoderm tissues. Posterior progenitors are known to co-express transcription factors related to neural and mesodermal lineages, e.g. Sox2 and Brachyury (Bra), respectively. In this study, we find that expression levels of Sox2 and Bra proteins display a high degree of variability among posterior progenitors of the quail embryo, therefore highlighting spatial heterogeneity of this cell population. By over-expression/down-regulation experiments and time-lapse imaging, we show that Sox2 and Bra are both involved in controlling progenitor motility, acting however in an opposite way: while Bra is necessary to progenitor motion, Sox2 tends to inhibit cell movement. Combining mathematical modeling and experimental approaches, we provide evidence that the spatial heterogeneity of posterior progenitors, with regards to their expression levels of Sox2 and Bra and thus to their motile properties, is fundamental to maintain a pool of resident progenitors while others segregate to contribute to tissue formation. As a whole, our work reveals that heterogeneity among a population of progenitor cells is critical to ensure robust multi-tissue morphogenesis.

Keywords: developmental biology, neuromesodermal progenitors, heterogeneity, cell motility, bird embryos, time lapse imaging, mathematical modeling, morphogenesis.

Introduction

Cells are the functional units of living organisms. During embryogenesis, they divide and specify in multiple cell types that organize spatially into tissues and organs. Specification events take place under the influences of the cell's own history and of environmental clues. Over the last years, access to new technologies has revealed that embryonic cells often display an unappreciated level of heterogeneity. For instance, gene expression analysis suggest that, within the same embryonic tissue, cells which were thought to be either equivalent or different, are actually organized into a continuum of various specification states (1,2). The impact of this new level of complexity on morphogenesis has not been extensively explored due to the difficulty of experimentally manipulating expression levels within targeted populations of cells *in vivo*. The progenitor cells located at the posterior tip of the vertebrate embryo (called here posterior progenitors) constitute a great model to study how a population of stem cell-like cells being specified into distinct cell types. The use of fluorescent tracers in bird and mouse embryos revealed that these progenitors contribute to the formation of the presomitic mesoderm (PSM), the mesodermal tissue that gives rise to the muscle and vertebrae, and of the neural tube the neuro-ectodermal tissue that gives rise to the central nervous system (3–6). These experiments have also shown that while some cells are leaving the progenitor zone, other progenitors remain resident in this area. Grafting experiments have later confirmed these properties by showing that these resident progenitors are indeed capable of self-renewal while giving progeny in different tissues (7,8). The posterior region therefore contains a population of different types of progenitors able to give progeny in the mesodermal or the neural lineages along the antero-posterior axis of the vertebrate embryo. Retrospective clonal analysis studies performed in the mouse embryo (9) confirmed heterogeneity of this progenitor population. Indeed, these studies revealed the existence of single progenitors able to give rise to only neural or mesodermal cells but also pointed out to the existence of a third type of progenitor able to generate both neural and mesodermal cells. These bi-potential progenitors, named neuro-mesodermal progenitors (NMPs), have later been shown to exist in zebrafish (10) and in bird embryos (48,50,51). In the early bird embryo (stage HH4-7), the future posterior progenitors are initially located in anterior epithelial structures: the epiblast and the primitive streak. At later stages (stage HH8 and onward), these progenitors are re-located caudally in the embryo in a dense mesenchymal structure that prefigure the embryonic tailbud where they will give rise to their progeny in the neural tube and PSM (48,(11)). To sustain the formation of tissues that compose the body axis, the posterior progenitor population must adopt an equilibrium between maintenance and specification/exit of the progenitor zone.

Two transcription factors, Sox2 (SRY sex determining region Y-box 2) and Bra (Brachyury), have been described for their roles in respectively neural and mesodermal specification during embryonic development (12,13). Sox2 is known to be expressed in the neural progenitors that form the neural tube where it contributes to the maintenance of their undifferentiated state. Its involvement in neural specification has also been revealed by a study showing that ectopic expression of Sox2 in cells of the presomitic mesoderm is sufficient to reprogram these cells, which then adopt a neural identity (14). The Bra protein was initially identified for its essential function in formation of the paraxial mesoderm during the posterior extension phase (12,15). Its crucial role in mesodermal specification has been demonstrated, in particular, by phenotypic study of chimeric mouse embryos composed of both Bra mutant and wild-type cells, and in which only wild- type cells are capable of generating mesodermal cells (16). More recent studies have shown that Sox2 and Bra proteins are expressed in posterior progenitors of developing embryos, indicating that activation of their expression takes place in progenitor cells before these cells colonize the neural tube or presomitic mesoderm (17,18). In addition, these studies have shown that both proteins are co-expressed in progenitor cells, an

observation consistent with the presence of bi-potential progenitors in this tissue. Work done in mouse embryo and *in vitro* systems derived from embryonic stem cells indicates that Bra and Sox 2 influence the choice between neural and mesodermal lineages by their antagonistic activities on the regulation of neural and mesodermal gene expression (19).

The purpose of this study is to understand further the relations between specification and tissue morphogenesis processes within the progenitor region of the developing vertebrate embryo. In particular, we want to investigate which cellular mechanisms can underlie maintaining enough progenitor cells while others are contributing to the elongating paraxial mesoderm and neural tissues. Analyzing the relative level of protein expression, we show that the specification factors Sox2 and Bra are expressed with a high degree of spatial heterogeneity in the progenitor region of the quail embryo. Over-expression and down-regulation experiments show that the ratio of Sox2/Bra expression is key in maintaining progenitors posteriorly and in controlling the exit of progenitor cells in their destination tissues. Using time-lapse experiments, we show that progenitor cells display diffusive migration properties comparable to PSM tissue. We developed a mathematical model to explore how heterogeneous expression of Bra and Sox2 combined with their opposite action on non-directional motility can drive both progenitor maintenance and multi-tissue morphogenesis. By overexpression and downregulation *in vivo* experiments, we further validate that Sox2 inhibits progenitor motility whereas Bra promotes it. Finally, by using our modeling approach we propose that spatial heterogeneity plays an important role in maintaining progenitor tissue shape during axial elongation.

Results

Levels of Sox2 and Bra proteins display high spatial cell-to-cell variability in the posterior zone.

The transcription factors Sox2 and Bra are known to be co-expressed in cells of the progenitor zone (PZ)(17,18). As they specify from these progenitors, neural cells maintain Sox2 expression and downregulate Bra while mesodermal cells downregulate Sox2 and maintain Bra. Although Sox2 and Bra are recognized to be key players in driving neural and mesodermal cell fates, the spatial and temporal dynamics of these events remains to be elucidated. As a first step to address this question, we carefully examined expression levels of the two proteins in the PZ of the quail embryo stage HH10-11. As expected, analyses of immunodetection experiments revealed co-expression of Sox2 and Bra in nuclei of most, if not all, PZ cells (Fig. 1 A-C) (n=8 embryos). Noticeably, we observed a high heterogeneity in the relative levels of Sox2 and Bra protein between neighboring cells. Indeed, in the progenitor zone, we found intermingled cells displaying high Sox2 ($Sox2^{high}$) and low Bra (Bra^{low}) levels or, conversely, Bra^{high} and $Sox2^{low}$ levels as well as cells in which both proteins appear to be at equivalent levels. This cellular heterogeneity was very apparent when compared to the adjacent nascent tissues, i.e. the neural tube and the PSM, where Sox2 and Bra protein levels were found to be very homogenous between neighboring cells (Fig. 1 D-F). We detected such cell-to-cell heterogeneity in progenitor as early as stage HH5-6, a stage corresponding to initial activation of Sox2 and Bra co-expression in the quail embryo (Supplemental Fig. 1). We also observed heterogeneous levels of Sox2 and Bra proteins in PZ cells of chicken embryo, indicating that it is not a specific feature of quail (Supplemental Fig. 2). To infer how Sox2 and Bra protein levels goes from being co-expressed in heterogeneous manner in the PZ to being expressed homogeneously in the nascent tissues we analyzed variations of their respective levels in a series of seven volumes (containing around 100 cells in each volume) located in a posterior to anterior path (from the PZ to the maturating tissues)

corresponding to PSM or neural tube putative trajectories (Figure 1G-G'). Data showed that expression level of Sox2 increases (+ 2.22 folds, n = 7 embryos) while that of Bra decreases (- 3.81 folds) following the neural path (Figure 1G). On the contrary, on the paraxial mesoderm path Sox2 level decreases (- 2.12 folds, n =7 embryos) while Bra level first increases in the posterior PSM (1.14 fold, position 1 to 2) and decrease later on (- 5.06 folds, position 2 to7) (Figure 1 G'). Next, to define whether the cellular heterogeneity found in the PZ depends more on variability of one of the two transcription factors, we quantified protein levels per nuclei of cells populating the PZ. By plotting Sox2 and Bra levels in individual cells we noticed a broader distribution for Sox2 levels (coefficient of variation of 41.8%) compared to Bra levels (coefficient of variation of 30.75%) (Fig 1 H), indicating that cell-to-cell heterogeneity in the PZ is preferentially driven by differences in Sox2 levels. To better quantify and visualize Sox2 and Bra heterogeneity we calculated the Sox2-to-Bra ratio (Sox2/Bra) for each cell of the PZ and compare it to neural tube and PSM. Comparison of Sox2/Bra values showed high divergences between the three tissues and confirmed the high heterogeneity previously observed in the PZ cells (Fig 1I). It must however be noticed that these quantitative data revealed a broad range of cell distribution, highlighting, in particular, the presence of cells in the PZ displaying similar Sox2/Bra values as mesodermal or neural cells. We next asked whether the cellular heterogeneity caused by differences in Sox2 and Bra levels is present in the whole volume of the PZ or displays regionalization in this tissue. To do so, we analyzed the spatial distribution of the same Sox2/Bra values on optical transverse sections performed at anterior, mid and posterior positions of the PZ (Figure 1J-J'''). This analysis confirmed that heterogeneous Sox2/Bra values are equally represented in the mid area of the PZ (Figure 1J''). Cells with a high ratio ($Sox2^{High}$ Bra^{Low}) were found to be more represented in the most dorso-anterior part of the PZ (Figure 1J') and cells with a low ratio (Bra^{High} $Sox2^{Low}$) were found to more represented in the most posterior part of the PZ (Figure 1J'''). This particular anteroposterior distribution was further confirmed by tissue expression analysis (Supplemental Fig. 3). However, variations of Sox2/Bra values were also noticed in these areas, indicating that cell-to-cell heterogeneity is present in the whole PZ.

Altogether, our data, highlighting significant variability in Sox2 and Bra protein levels within progenitors of the PZ, evidence an unexpected cell-to-cell heterogeneity of this cell population. Noticeably, despite an overall enrichment of $Sox2^{high}$ cells in the dorsal- anterior part of the PZ and Bra^{high} cells in the most posterior part, no clear spatial regionalization of these cells was detected, indicating that the PZ is composed of a complex mixture of cells displaying variable Sox2/Bra levels. This variability is further lost as cells enter the neural tube or the PSM.

Relative levels of Sox2 and Bra in PZ cells influence their future tissue distribution.

The fact that cell-to-cell heterogeneity caused by differences in the Sox2 and Bra levels is observed in PZ cells but not in PSM and the neural tube cells is suggestive of a role of these relative protein levels in the decision to leave or not the PZ and to locate in a specific tissue. To test this possibility, we developed functional experiments aiming at increasing or decreasing Sox2 and Bra levels in PZ cells. To do this, we performed targeted electroporation of progenitors in the anterior primitive streak/epiblast of stage HH5 embryos to transfect expression vectors or morpholinos and further analyzed subsequent distribution of targeted cells, focusing on the PZ, the PSM and the neural tube (Figure 2). As early as 7hrs after electroporation, we could detect the expected modifications of Sox2 or Bra expression in PZ cells for both overexpression and downregulation experiments (Supplemental Figure 4,5). We observed a significant decrease in the Sox2/Bra levels either by overexpressing Bra or downregulating Sox2 while this value increased when Sox2 is overexpressed or when Bra is downregulated (Figure 2 A,F). Consistent with previous studies (19), we found that cross-repressive

activities of Sox2 and Bra contributed to amplify such ratio's modifications (Supplemental Figure 5). After transfection of expression vector or morpholino, we let the embryos develop until stage HH10-11 and examined fluorescent cell distribution in the different tissues. For this, we measured the fluorescence intensity of the reporter protein (GFP) in the PZ, the PSM and the neural tube and calculated the percentage of fluorescence in each tissue. We obtained reproducible data using control expression vector with less than 20% of the fluorescent signal found in the PZ (16.78% ±2.83), a little more than 20% in the PSM (22.64 % ± 3.30) and about 60% in the neural tube (60.57% ± 4.39) (Figure 2 B, E). We next found that overexpression of Bra leads to a marked reduction of the fluorescent signal in the PZ (1.17% ± 0.57) and to an increased signal in the PSM (33.04% ± 4.06) but has no effect on the neural tube signal (Figure 2 C, E). Elevating Bra levels is thus sufficient to trigger cell exit from the PZ and to drive cells to join the PSM. However, this is not sufficient to impede PZ cell contribution to form the neural tube. Similarly, we found that overexpression of Sox2 drives exit of the cells from the PZ (1.16% ± 0.67) favoring their localization in the neural tube (75.40% ± 4.57) without significantly affecting proportions of cells in the PSM (Figure 2 D,E). Spatial distribution of the fluorescent signals obtained using control morpholinos appeared very similar to that observed using the control expression vector (18.93% ± 3.06, 22.68 ± 4.09 and 58.38% ± 3.63 for the PZ, the PSM and the neural tube, respectively). We found that downregulation of Bra leads to exit of cells from the PZ (4.16% ± 1.57), favors cell localization in the neural tube (88.23%, ± 2.04) at the expense of the PSM (7.59% ± 1.81) (Figure 2 G, H, J). Similarly, Sox2 downregulation trigger cell exit from the PZ (7.50% ± 2.35) and, as expected, leads to higher contribution of cells to the PSM (34.59% ± 4.79) but this does not occur at the expense of cell contribution to the neural tube (Figure 2 G, I, J).

These data thus point out that the relative levels of Sox2 and Bra proteins are key determinant of PZ cell choice to stay in the PZ or leave it to enter more mature tissues. Major changes of the Sox2 to Bra ratios, tending either towards higher or lower values, are sufficient to trigger cell exit from the PZ. These experiments also pointed to the critical influence of the relative levels of Sox2 and Bra in controlling the final destination of cells exiting the PZ, with $Sox2^{high}$ (Bra^{low}) cells and Bra^{high} ($Sox2^{low}$) cells preferentially integrating the neural tube and the PSM, respectively. Intriguingly, we also observed that the preferential cell colonization of one given tissue is not always clearly associated with depletion of cells in the other (see discussion).

PZ cells are highly motile without strong directionality

To have a better understanding of how progenitors either stay or leave the PZ we needed to study their behavior dynamically using live imaging. We electroporated stage HH5 quail embryos with an empty vector encoding for nuclear GFP and preformed time-lapse imaging was further performed from stage HH8 to stage HH12. We focused our interest on the PZ but also on the PSM and the posterior neural tube in order to be able to compare migration properties between tissues (Figure 3A, Supplemental Movie 1). Because these three tissues have a global movement directed posteriorly due to the embryonic elongation, we generated two types of cellular tracking: the raw movement, in which the last formed somite is set as a reference point and the "corrected" movement, in which the cellular movements are analyzed in reference to the region of interest (Figure 3B). Tracking cell movements allowed for quantification of motility distribution, directionality of migration and time-averaged mean squared displacement (Figure 3C-E) (n=7 embryos). First, we noticed that PZ cell raw motilities are higher than that of PSM or neural tube cell motilities (Figure 3C, top panel). PZ raw directionality is also more pronounced in the posterior direction (Figure 3D, upper panel). These results confirm that the PZ is moving faster in a posterior direction than surrounding tissues as previously measured using transgenic quails embryos (20). Analysis of local (corrected) motility reveals that PZ cells move globally

as fast as PSM cells and significantly faster than neural tissue cells (Figure 3C, bottom panel). The distribution of corrected PZ cell motilities is however different to the one of PSM cells as it showed slower moving cells (PZ corrected motility violin plot in Figure 3C is larger for slow values than the PSM counterpart and Supplemental Figure 6). After tissue correction, the directionality of PSM cell motion was found mostly non-directional as previously described (20) with a slight anterior tendency which is expected for a posteriorly moving reference (Figure 3D, red plot in the lower panel). The distribution of corrected angles of PZ cell motilities is also globally non-directed with the exception of a slight tendency toward the anterior (to some extent more than the PSM cells), suggesting that our method is able to detect trajectories of cells exiting the region of interest (Figure 3D, yellow plot lower panel). As PZ cell movement was found being mostly non-directional, we wanted to better characterized their diffusive motion by plotting their mean squared displacements (MSD), measured in each tissue over time, as it has been previously done for PSM cells (20). This analysis showed that progenitor MSD is linear after tissue subtraction, as intense as the PSM cell MSD and significantly higher than neural tube cell MSD, thus demonstrating the diffusive nature of PZ cell movements (Fig. 3E).

Together, these data evidenced that, in the referential of the progenitor region, PZ cell migration is diffusive/without displaying strong directionality (expect a slight anterior tendency), with an average motility that is comparable to PSM cells and significantly higher than that of neural tube cells.

Modeling spatial cellular heterogeneity and tissue morphogenesis

To understand better how heterogeneity in Sox2/Bra can control the choice of progenitors to stay or leave the PZ we designed an agent based mathematical model (Figure 4). The main hypothesis of this model is that motility in a given progenitor is directly driven by the Sox2/Bra value; Bra is promoting non-directional motility whereas Sox2 is inhibiting it. We chose some initial conditions in which the neural tube, the PSM and the axial progenitor are already formed. This choice was motivated by the fact that our experiments focus on a developmental window, which is passed the formation of these tissues (HH8-HH12). At this period of development the main tissues deformations are in the antero-posterior and medio-lateral axis (21), thus we decided to design a 2D model (X,Y) evolving through time. We implemented cell numbers, proliferation, and tissue shape to be as close as possible to biological measurements (21) (Supplementary data). We set up the PZ cells to express random and dynamic Sox2/Bra levels with a defined probability to switch into a Sox2 ^{high}(Bra ^{low}) state (neural tube state) or a Bra ^{high}(Sox2^{low}) state (PSM state) (Figure 4A). To take into account our biological observation that PZ cells are as motile as PSM cells we set up the threshold at which the motility is switching from high to low at a Sox2/Bra level of 1.6 (the level above which cells become committed to neural fate). Finally, to consider the physical boundaries existing between tissues, we integrated a non-mixing property between cell types. We first verified that our mathematical model (Supplemental Movie 2) recapitulates the basic properties of the biological system: in particular, it allows for recreating spatial heterogeneity of relative Sox2/Bra levels in cells of the PZ (Figure 4B) and reproduces general trends in tissue motility and non-directionality (Figure 4C,D). Simulations of our model also showed that relative cell numbers (taking into account proliferation) evolve as expected with a stable number of PZ cells and an increase in neural tube and PSM cells (Figure 4E). To check if spatial heterogeneity of Sox2/Bra levels can self-organized in our model we made a simulation in which every progenitor start with equivalent levels of Sox2 (50%) and Bra (50%). We observed that spatial heterogeneity was emerging after few time-points and persisting all along the simulation suggesting that this feature is indeed able to self-organize independently of the initial levels of Sox2/Bra (Supplemental Movie 3). We next explored the model's ability to reproduce maintenance of progenitors and elongation of posterior tissues during the elongation process. By looking at different time points in the simulation, we observed that the progenitor region stays posterior to the neural tube. Neural tube and paraxial

mesoderm both extend posteriorly (Figure 4F, Supplemental Movie 2). These results show that our mathematical model is able to reproduce the main properties of our biological system. Interestingly, simulations also showed dynamic deformation of the progenitor region, which adopts asymmetric shapes and then gets back to symmetric, thus highlighting self-corrective properties of the system. To challenge further this model and test if it can recapitulate the experimental results we obtained by over-expression and down-regulation of function of Sox2 and Bra we explored the consequences of numerically deregulating the Sox2/Bra values on tissue and cell behavior. As a result, Bra^{High} values increase PZ cell motility in the model (Figure 4G), lead to more PSM cells (Figure 4H), a depletion of cells in the PZ and a shorter neural tube (Figure 4H,J Supplemental Movie 4). At the opposite, $Sox2^{High}$ values leads to a reduction of PZ cell motility (Figure 4G), depletion of PZ cells and an increase of neural tube cells (neural tube shows an enlargement) at the expense of PSM cells (Figure 4I,J Supplemental Movie 5). The results of our numerical simulations are therefore coherent with our experimental data showing that Sox2/Bra levels control the balance between maintenance of progenitors in the PZ and continuous distribution of cells into the neural tube and the PSM. Together, the results obtained by our model strongly suggest that progenitor behavior can be guided by creating Sox2/Bra-dependent heterogeneous cell motility.

Sox2 and Bra control motility of PZ cells

Our mathematical model suggests that the control of cellular motility by Sox2/Bra levels is critical to influence progenitor behavior (staying or leaving the PZ to go to the neural tube or the PSM). To test this prediction we needed to define whether Sox2 and Bra are indeed involved in controlling progenitor motility *in vivo*. Therefore, we proceeded to over-expression and down-regulation experiments followed by time-lapse imaging in quail embryos (Figure 5 A-F). We focused on monitoring the PZ to define how cells behave in this region, either staying or leaving this tissue. As for control embryos (Figure 3), we first monitored raw cell motilities (Supplemental Figure 7) and conducted subtraction of the tissue motion to gain insight into local motility and directionality (Figure 5). We found that Bra-overexpressing PZ cells display higher motility without significant differences in directionality when compared to control embryos. By contrast, when PZ cell overexpress Sox2, we detected a significant reduction of their motility compared to control accompanied by an anterior bias in angle distribution (Figure 5 B,C,D, Supplemental Movie 6). Bra down-regulation leads to similar significant reduction of cell motility, as well as a change in directionality toward the anterior direction 6. Conversely, Sox2 down-regulation did not result in significant effect on average cell motility or directionality, even though a tendency towards a slight increase in motility was noticed. (Figure 5 B,E,F, Supplemental Movie 7).

These data, showing that changing the respective levels of Sox2 and Bra is sufficient to modulate PZ cell motility/migration properties, highlight a key role for these transcription factors in controlling PZ cells movements with Sox2 and Bra inhibiting and promoting cell motility, respectively. In that sense, these results validate the importance of the regulation of motility by Sox2/Bra levels hypothesized by our mathematical model. When cells have high Sox2/Bra levels they migrate less and are left behind the PZ to be integrated in the neural tube. When cells have a low Sox2/Bra ratio they tend to migrate more, mostly in a diffusive manner, explaining how they leave the PZ to be integrated in the surrounding PSM tissues.

Modeling the importance of spatial heterogeneity in morphogenesis.

Our experimental and theoretical data point out that heterogeneity in Sox2 and Bra expression are key to control progenitor behaviors during axis elongation. However, we still do not know the importance of the spatial randomization of this heterogeneity (the fact that we observe very different Sox2/Bra levels in neighboring cells without clear pattern) in comparison to a heterogeneity that is spatially organized. To assess this particular point, we created a second mathematical model in which Sox2 and Bra levels, instead of being randomly distributed, are simply patterned in two opposite gradients as we have observed in the dorsal part of the PZ (Figure 6A, Figure 1 J, and Supplemental Figure 3). In this area, Sox2 was found displaying an antero-posterior decreasing gradient while Bra displays an opposite antero-posterior increasing gradient. This new version of the model has been set up to reproduce similar dynamics in cell specification (Figure 6B) and relationships between Sox2/Bra and motility as in the previous model (Supplemental methods). We observed that the motility of the PSM, and PZ of the gradient model are globally comparable to the spatially heterogeneous model (Figure 6C, 4C) and mostly non-directional (Supplemental Figure 8). We observed maintenance of PZ cells caudally and elongation of the different tissues (Figure 6D, Supplemental Movie 8) suggesting a gradient in Sox2 and Bra expression can also explain progenitor maintenance and distribution. Despite the observed similarities, we noticed several crucial differences between our heterogeneous and our biologically inspired gradient model. Indeed, the speed of elongation is less important in the graded simulation (0.8 a.u.) versus the spatially heterogeneous simulation (1.2 a.u.) (Figure 6E). To check if, at the cellular level, resident progenitors are displaced differentially in the posterior direction between the two models we tracked cells at the center of the PZ and calculated the distances they travelled in the Y direction. Analysis showed resident progenitors move more posteriorly in the heterogeneous (mean distance of 3.37 a.u.) versus the gradient model (mean distance of 3.18 a.u.) suggesting that the heterogeneous model is more efficient at maintaining resident progenitor posteriorly (Figure 6F). We also noticed less transient deformations and self-corrective behavior of the PZ in the gradient simulation when compared to the heterogeneous simulation (Supplemental Movie 9). By analyzing the PZ shape on longer time scales (beginning to end of the simulation) in each model, we found that, the shape of the PZ changes considerably in the gradient simulation. Indeed, it became larger (medio-lateral) and shorter (antero-posterior), showing less conservation of proportions 41% (gradient) vs 86% (heterogeneous) (Figure 6G). Finally, to test if the changes we observed could be due changes in the diffusivity of cellular migration we plotted the MSD through time for each of the models. We found that the MSD of the spatially heterogeneous model is higher that the gradient model (Figure 6H) suggesting that the spatial heterogeneity in expression of Sox2 and Bra is enhancing the diffusive behavior of the PZ cells. This higher diffusivity can therefore bring more fluidity in the tissue in order to remodel more efficiently and to maintain its shape on longer time scales and allow for more posterior displacements of resident progenitors. Together, data obtained from our mathematical models argue in favor of spatial cell-to-cell heterogeneity being able to create an appropriate balance between two possible decisions for a PZ cell, i.e. staying in place or going away to contribute to adjacent tissues. Moreover, it argues that spatial cell-to-cell heterogeneity is important to allow tissue fluidity and remodeling in order to maintain PZ shape during axial elongation.

Discussion

Our results reveal the existence of spatial heterogeneity in expression levels of Sox2 and Bra proteins in the posterior progenitors of bird embryos. Experimental and theoretical approaches converge toward the point that spatial heterogeneity of Sox2/Bra ratio play essential roles in regulating progenitor maintenance and their allocation to the neural tube or PSM through the control of cellular motility. Altogether, our data lead us to propose the following working model. Progenitor cells

expressing intermediate levels of Sox2 and Bra stay motile and remain resident within the posteriorly moving progenitor tissue. Cells expressing high levels of Sox2 reduce their motility and therefore are forced to leave the progenitor zone to integrate in the neural tube, while progenitors expressing high level of Bra "diffuse" more actively than other progenitors and exit the PZ to integrate the PSM. This model shed new light on how specification and morphogenesis is coupled during vertebrate embryo axis elongation and highlights the fact that heterogeneity can be a beneficial feature to ensure robustness in morphogenesis.

The fact that we can detect different levels of Sox2 and Bra expression between progenitors is indicative that axial progenitor cells are in different specification states, some progenitors are more engaged toward the mesodermal fate, some toward the neural fate while others are still in between these states. These different specification states could explain why in our gain and loss-of-function experiments preferential distribution of electroporated cells in the neural tube is not always paralleled by a decrease in participation in the PSM (or inversely) (Figure 2E, J). Indeed a progenitor, which is for instance, already engaged toward a neural fate, might not be competent to become mesoderm anymore and might follow its path toward neural tube even if experiencing a sudden rise in Bra level. Single cell sequencing of the progenitor region of mouse embryos have revealed that different types of specification states co-exist within posterior progenitors (19). It is likely that the different states that we observe by visualizing different Sox2/Bra proteins ratio is also defined by differential gene expression of mesodermal and neural genes. To test this hypothesis further it would be interesting to analyze other neural and mesodermal genes and test if they have heterogenic pattern of expression in the progenitor region. Due to its technical limitation, single cell studies does not reveal the exact locations of the different progenitor states found within the posterior region. The first heterogeneity that we have observed is patterned spatially in a gradient along the antero-posteriorly axis (Sox2 high anteriorly, Bra high posteriorly) in the dorsal part of the region. This graded expression has been described in chicken embryo (22)(49) and is coherent with fate maps studies at earlier stages showing that the antero-posterior axis of the epiblast/streak gives rise to progeny along the medio-lateral axis (4,6). For instance, anterior cells expressing high levels of Sox2 can give rise to neural cells and more posterior cells expressing high levels of Bra to PSM (and eventually to lateral mesoderm to cells located even more caudally). However, our analysis also reveals a spatial heterogeneity between neighboring cells in the progenitor region (dorsally and ventrally). This finding is suggestive of a more complex picture where position in the progenitor region do not systematically prefigure final tissue destination. In this case, Sox2/ Bra ratio would be determinant in assigning progenitor fate independently of the initial position. This scenario involve much more cell mixing and could participate in explaining why prospective maps of this region have shown multi-tissue contribution (3–6). In our functional experiments aiming at biasing PZ cells toward neural state (Pcig-Sox2, Bra-Mo) we have stronger effects in motility and tissue distribution than in experiments in which we aim at biasing PZ cells toward mesodermal fate (Pcig-Bra, Sox2 Mo). These differences can be explained and reinforced by our finding that the motilities of PZ cells are much more similar to PSM motilities than to neural tube. Therefore, a change of progenitor behavior toward a neural tube behavior is much likely to affect motility and progenitor distribution than a change toward a mesodermal state.

The action of graded signaling pathways such as Wnt, FGF and RA have been described to positively regulate the expression of Bra and Sox2 genes and to affect progenitor destiny (23–30). It will be necessary and useful to test whether these pathways regulate Sox2 and Bra in posterior progenitors of quail embryos. However, no data allow us to say that the activity of these signaling pathways is sufficient to explain the spatial heterogeneity that we observed between neighboring cells in this region. Our data, as well as data from the literature, suggest the existence of a mutual repression mechanism of Sox2 and Bra in posterior progenitors (Supplemental Figure 5 and (19)). The expression

of these transcription factors could therefore be controlled positively through signaling pathways and negatively by cross-inhibition activities. This synergy between signaling and cross-repressive activity could therefore allow for a temporal dynamic responsible for the spatial heterogeneity we observe. In our mathematical model, we propose that the expression of Sox2 and Bra is spatially and temporally dynamic within progenitors. This hypothesis needs to be investigated with specific reporter and live imaging. However if true, one could postulate that a progenitor that oscillate between a high Bra low Sox2 state and a low Bra high Sox2 state give rise to progeny in the neural or mesodermal lineages depending on these ratios at the moment of cell division. Studies in mouse and recent studies in birds suggest that a single progenitor clone (true NMP) can give rise to progenies in the neural tube and the paraxial mesoderm (9). Interestingly, the authors observe that the final positions of these progenies are different along the antero-posterior axis suggesting a sequential production: progenitor cells give rise to mesoderm and then switch to neuroectoderm (or the opposite). An oscillation between cellular specification states of the NMP could therefore be a possible explanation to these observations.

Recent studies have shown that during the course of axis elongation axial progenitor cells undergo an EMT before reaching their full potential and give rise to progeny in the neural tube and the paraxial mesoderm (23,31)(48). We observe that, if analyzed between stage HH5 and HH8, the progenitor region displays a low range of local movements in comparison to stages HH8 to HH11 (data not shown). Therefore, it is likely that local motility is very low when progenitors are still epithelial and become high and non-directional when the progenitors become more mesenchymal and are relocated caudally. However, it is interesting that even if the tissue is more mesenchymal at later stages it keep its global posteriorly directed tissue motion. Works in bird embryo have shown that the posterior movement of the progenitor zone is the result of physical constrains exerted by the neighboring tissues PSM and neural tube (21,32). PSM expansion can indeed exert pressure on axial tissues generate a general posterior movement of the progenitor zone. Our data indicate that the range of cellular motility of progenitors belonging to this moving region is key in determining their fate, high Bra expressing cells move actively and leave the region laterally whereas high Sox2 cells move less, and are left behind in the neural tissue. In our experiments, over-expression of Sox2 and down-regulation of Bra leads to an anterior bias in the direction of progenitor movements. However If we consider the posteriorly moving progenitor region, this would correspond to an absence of movement for neural progenitors. Indeed, it has been proposed that the progressive depletion of progenitors committed toward the neural fate occurs without excessive cell mixing (33) and therefore could not require active migration. Although the role of Sox2 on progenitor cell migration has, to our knowledge, never been described, recent work has demonstrated that Sox2 is implicated in the transition from neural progenitor to neural tube during chick embryo secondary neurulation (22). Concerning Brachyury, it has been previously shown that this transcription factor has a role in cell migration. Mouse cells that have a mutation in the Brachyury gene have lower migration speed than wild type cells when isolated and cultured, explaining part of the mouse embryonic phenotype (34). The molecular mechanisms that act downstream of Sox2 and Bra to promote or inhibit cell migration are still to be discovered.

From the result of our mathematical models, we can propose that both a spatially random and a patterned heterogeneity in Sox2 and Bra expression are able to maintain progenitors caudally and to guide their progeny in the neural tube and mesoderm. In our biological system we observe a superposition of spatially randomized and a patterned distribution of Sox2/Bra levels. It is therefore tempting to suggest that both systems (spatially random and gradient) are at work in the embryo. Interestingly, little is known about the role of spatial heterogeneity in morphogenesis. We propose that this random pattern allow for more cell rearrangements/tissue fluidity in the progenitor zone. This fluid like state and the opposite solid like state of the anterior PSM tissue have been shown to be key for zebrafish embryo axis elongation (35,36). Furthermore, the fact that we observe more self-

correction in our model also suggests that spatial heterogeneity can provide plasticity to the system. Interestingly, several studies have shown that this particular region of the embryo is able to re-generate after deletion of some of its parts (37,38). In that regards, spatial heterogeneity could be easily re-organized in remaining cells in comparison to gradients. Indeed, if gradients of Sox2 and Bra are controlled by secreted signals, one could imagine that the absence of tissue could be more detrimental to the diffusion of this signal and therefore to re-patterning. Spatial heterogeneity in gene and protein expression is a common trait of living system and has been found in many contexts including cancer cells (39). The link between cellular spatial heterogeneity and the robustness of morphogenetic processes that we describe can therefore be relevant beyond the scope of developmental biology.

Material and Methods

Quail Embryos and cultures:

Fertilized eggs of quail (Coturnix japonica) obtained from commercial sources, are incubated at 38°C at constant humidity and embryos are harvested at the desired stage of development. The early development of quail being comparable to chicken, embryonic stages are defined using quail (40) or chicken embryo development tables (41). Embryos are grown *ex ovo* using the EC (early chick) technique (42) 6 to 20 hours at 39°C in a humid atmosphere.

Expression vectors and morpholinos:

cBra full length cDNA was cloned by PCR using the following primers (5'-ACCATGGGCTCCCCGGAG-3'; 5'-CTACGCAAAGCAGTGCAGGTGC-3') into Pcig (43). cSox2 was cloned from Pccags-cSox2 (gift from Daniela Roellig (44)) using EcoRV/XbaI into Pcig to obtain Pcig-cSox2. Fluorescein-coupled morpholinos were synthesized by Gene Tools. The nucleotide sequences of the morpholinos were chosen to target the translation initiation site of quail Bra (5'-AAATCCCCCCCCCCTTCCCCGAG-3') and quail Sox2 (5'-GTACATTCAAACTACTTTTGCCTGG-3') mRNAs. The Mo control (5'-CCTCTTACCTCAGTTACAATTTATA-3') is directed against the transcript of β-human globin.

Electroporation :

We collected stage 4-6 quail embryos. The solution containing the morpholinos (1mM) and pCIG empty (1-2µg/µL) as a carrier or the DNA solution containing expression vectors Pcig , pCIG-Bra or pCIG-Sox2 (2-5µg/µL) were microinjected between the vitelline membrane and the epiblast at the anterior region of the primitive streak (45). The electrodes were positioned on either side of the embryo and five pulses of 5.2V, with a duration of 50ms, were carried out at a time interval of 200ms. The embryos were screened for fluorescence and morphology and kept in culture for up to 24 hours.

Fluo- and immunofluorescence :

For immunodetection embryos of stages HH 9 to HH11 were fixed for 2 hours at room temperature in formaldehyde 4% in PBS. Blocking and permeabilization were achieved by incubating the embryos in a solution containing Triton X-100 (0.5%) and donkey serum (1%) diluted in PBS for 2 hours. The embryos were then incubated with primary antibodies to Sox2 (1/ 5000, EMD Millipore, ab5603) and Bra (1/500, R&D Systems, AF2085) overnight at 4°C under agitation. After washes the embryos were incubated with secondary antibodies coupled with AlexaFluor555, AlexaFluor488 (1/1000,

ThermoFisherScientific) and DAPI (4',6-diamidino-2-phenylindole, 1/1000, ThermoFisherScientific D1306) overnight at 4°C with agitation. To observe the distribution of fluorescence in electroporated tissues embryos were cultured overnight and fixed before being mounted ventral side up.

Image acquisition and processing:

Image acquisition for immunodetection was performed using a Zeiss 710 laser confocal microscope (20x and 40x objectives). Quantification of Sox2 and Bra levels in 3D have been made with Fiji or with the spot function (DAPI Staining) of Imaris. Expression have been normalized to DAPI to take into account loss in intensity due to depth, expression and ratios have been calculated and plotted using Matlab. Protein expression after gain and loss of function experiments has been done 7 hours after electroporation by analysing immunodetection signal levels within GFP positive progenitors and normalizing to endogenous expression. Fluorescence distribution in tissues has been acquired on a wide field microscope Axio-imager type 2 (Colibiri 8 multi-diode light source, 10X objective). The images of electroporated embryos were processed with the Zen software that allows the assembly of the different parts of the mosaic ("Stitch" function). The images were then processed with the "Stack focuser" plugin of the Image J software. The different tissues were delineated on ImageJ with the hands-free selection tool and then the images were binarized using the threshold tool. The total fluorescence intensity emitted for the cells transfected with the different constructs were measured and the sum of the positive pixels for the different tissues was calculated. The percentage distribution of fluorescence in the different tissues was then calculated.

Live imaging and cell tracking

Live Imaging has been done using Zeiss Axio-imager type 2 (10X objective) and was described here (31). Briefly, stage 7-8 electroporated embryos were cultured under the microscope at 38 degrees under humid atmosphere. Two channels (GFP and brightfield), 3 fields of views, 10 Z levels have been imaged every 6 minutes for each embryo (6 embryo per experiments). Images were stitched and pixels in focus were selected using Stack Focuser (ImageJ). X, Y drift was corrected using MultiStackReg adapted from TurboReg (ImageJ) (46). Image segmentation was done after background correction using Background Subtractor plugin (from the MOSAIC suite in ImageJ) and cell tracking was done using Particle Tracker 2D/3D plugin (ImageJ) (47). A reference point was defined for each frame at the last formed somite using manual tracking. Region of interest were defined manually and their posterior movement was defined by manual tracking of the tailbud movement. Subtraction of the tissue movement was done by defining the average motions of cells in the region. Violin plots were generated on Prism 8 (Graphpad). MSD and distribution of angles were calculated and plotted with a Matlab routine. Angle distribution was calculated from trajectories, weighted with velocities and plotted as rosewind plot using Matlab.

Statistical testing:

Kolmorogov-Sminorv test has been used to test for differences in angle distributions in Figure 5D and 5F. For all the other comparison unpaired Student test have been used. ($P<0.05$ *, $P<0.001$ **, $P<0.0001$ ***, $P<0.00001$ ****, $P>0.05$ ns (non-significant))

Mathematical modeling

We initially distribute 1100 progenitor cells, 1200 neural cells, and 3200 PSM cells, randomly in their respective areas. Each cell type is endowed with its proliferation rate: 11.49 hours for the progenitor cells, 10.83 hours for the neural cells and 8.75 hours for PSM cells. Each cell I is characterized by its

ratio of Sox2/Bra R_I(t) between 0 and 1 (depicted as 0-2in Figure 4A to match with biological ratios) and its position in 2D (x_I(t),y_I(t)), each of these variables is time-dependent. In the heterogeneous case, we initially randomly attribute a ratio between 0.15 and 0.85 to the progenitor cells. At each time step, these cells update their ratio through a first order ODE using the function represented in Figure 5A (+ noise), and then update their position (x,y), depending on their ratio, by a biased/adapted random motion. Interaction properties between cells such as adhesion, maximum density, packing are implemented in the bias of the random motion, as detailed in the Supplementary Materials and Methods. In the simulations we represent a portion of the posterior body (1 unit=150 micrometers), block the movements of the cells in the most anterior region as we consider it a very dense area (somites, epithelium neural tube), and block their passage to either side of the PSM as we consider the lateral plate to be a solid structure.

Acknowledgements:

We thank Karine Guevorkian, Eric Theveneau, and Myriam Roussigné for critically reading the manuscript. We thank Brice and Stephanie of the CBI imaging facility and Marion Aguirrebengoa for help with statistics. We also thank members of the Pituello, Soula, Theveneau and Davy teams for suggestions and stimulating discussions during the project.

Competing interests:

The authors declare no competing or financial interests.

Figure legends

Figure 1: Progenitors co express Sox2 and Bra with a high degree of cell-to-cell heterogeneity.

A-F : Sox2 (green) and Bra (red) expression has been analyzed at the cellular scale in the caudal part of stage HH11 quail embryo, either in the progenitor region (**A-C**) or in the nascent neural tube and PSM (**D-F**). Overlay images are presented in **C** and **F**. Note that cell-to-cell heterogeneity in Sox2 and Bra levels are apparent in the progenitor region, with neighboring cells having higher Bra (red arrow), higher Sox2 (green arrow) expression levels or both proteins at similar levels (yellow arrow) which is

not apparent in the nascent neural tube and PSM tissues. **G, G'**: Levels of Sox2 and Bra in different embryonic locations corresponding to neural tube maturation (**G**) and paraxial mesoderm maturation (**G'**). Images on the left display locations for the measurements (blue squares), charts on the right display the different levels measured. **H**: Distribution of normalized cell-to-cell expression for Sox2 and Bra in the progenitor region (n=8 embryos). Coefficient of variation are more important for Sox2 (41.48%) than for Bra (30.75%). **I**: Cell distribution of Sox2/Bra levels in the progenitor zone (n=9 embryos), the neural tube (n=7 embryos) and the PSM (n=8 embryos). **J-J'''**: Representation of the Sox2 and Bra ratio (green to red) in digital transversal sections (40 µm) made in the progenitor region (dashed lines in the double immunodetection image in **J**). Scale bars represent 10 µm for **A-F**, 100 µm for **I,L,L'.**

<u>Figure 2</u>: Sox2 and Bra levels are critical for progenitor maintenance and tissue distribution.

Sox2-Bra ratios have been analyzed by double immunostaining in the progenitor zone 7 hours after electroporation and normalized to the average ratio of non-transfected cells of the same region (**A,F**). **A** Overexpression of Pcig-Bra and Pcig-Sox2 compared to empty vector (Pcig). **B** Morpholinos experiments Bra Mo, Sox2 Mo compared to control Mo. Ratio have been calculated for 286-590 cells and 3-5 embryos per condition. Images of the GFP signals (white) of posterior regions of embryo (ventral view) collected 20hrs after electroporation (**B-D, G-I**). The yellow dash line delineates the progenitor regions, the red dashed line delineate the PSM regions and the green dashed line delineate the neural tube tissues. In **B,C,D** are displayed an image of an embryo with overexpression of Pcig, Pcig-Bra and Pcig-Sox2 respectively. In **G,H,I** are displayed images of embryo with electroporation of Control Mo, Bra Mo and Sox2 Mo respectively. The white bar in B represents 100 µm; all images have been taken at the same magnification. **E** and **L** are staked histograms displaying the proportions of cells in each tissues (yellow is the progenitor zone, red is the PSM, green the neural tube). Proportions for each tissue have been compared to control experiment by unpaired Student test. (Errors bars represent the SEM, n= 27 embryos for Pcig Bra, n= 21 embryos control for Pcig, n=23 embryos for Pcig Sox2; n=28 embryos for Bra Mo, n=27 embryos for Control Mo, n=28 embryos for Sox2 Mo).

<u>Figure 3:</u> Progenitors display high motility without strong directionality.

Live imaging analysis of H2B-GFP electroporated quail embryos. **A.** Image showing a ventral view of the posterior region in a representative embryo (left panel). GFP signal is in green, region of interest are delineated as follow: yellow for the progenitor, red for the nascent paraxial mesoderm and green for the neural tube. **B**: Example of cellular trajectories in the different regions before (raw) and after tissue motion subtraction (corrected). **C**. Distribution of the cellular motilities computed in the different region of interest. On the top panel raw motility and bottom panel corrected motilities. **D**. Directionality of motion assessed by the distribution of angles weighed by the velocity for the different regions of interest, before and after tissue subtraction. **E.** Assessment of diffusion by analysis of the mean squared displacement in function of time for the different region of interest. (n=7 embryos, 538 trajectories analyzed for the progenitor region, 496 for the paraxial mesoderm, 128 for the neural tube). Scale bar is 100 µm.

<u>Figure 4:</u> Mathematical modeling of posterior progenitor behavior downstream of heterogeneous expression of Sox2 and Bra.

A: Graphical representation of the mathematical function defining the ratio Sox2/Bra dynamics. In each progenitor cell, Sox2/Bra ratio oscillates randomly between 0.4 and 1.6, noise in the system ensures that some cells pass below 0.4 to specify into paraxial mesoderm (red) and some cells pass above 1.6 to become neural tube (green). Medium and low ratios (below 1.6) confer high-motility, high ratios (above 1.6) inhibit motility. **B:** Progenitor region showing the spatial heterogeneity of Sox2/Bra

levels with a close up on the PZ on the bottom panel. **C**: Distribution of motilities within the progenitor zone (PZ), PSM and neural tube (NT). **D**: Directionality of migration on the three tissues. **E**: Evolution of cell numbers for each cell type. **F:** Evolution of the model through different time points 0, 5hrs and 10 hrs. Note that the tissues are preformed at time 0, PSM is in red, neural tube in green and PZ in yellow. Black bar show the elongation rate. **G**: Distribution of motilities within the progenitor zone (PZ), for low Sox2/Bra (high Bra) or high Sox2/Bra (high Sox2) compared to control; **H**: Evolution of cell numbers for each cell type for low Sox2/Bra (high Bra). **I**: Evolution of cell numbers for each cell type for high Sox2/Bra (high Sox2). **J**: Evolution of the model at 5hrs low Sox2/Bra (high Bra) (right panel) or high Sox2/Bra (high Sox2) (left panel) compared to control conditions (middle panel).

Figure 5: Sox2 and Bra overexpression and downregulation affect progenitor motility

Progenitor tracking and motility analysis for Sox2 and Bra overexpression and down regulation. **A**: Image showing a ventral view of the posterior region in a representative embryo, GFP signal is in green, region of interest (PZ) is delineated in yellow. **B**: Examples of track after correction in the different experimental conditions**.** Distribution of the cellular motility in the progenitor zone after tissue motion subtraction for gain of function experiments (**C**), and down-regulation (**E**). Directionality of motion after tissue motion subtraction assessed by the distribution of angles for gain of function experiments (**D**), and downregulation (**F**). (n=7 embryos and 541 trajectories for Pcig, n= 5 embryos and 307 trajectories for Pcig-Bra, n= 5 embryos and 234 trajectories for Pcig-Sox2; n=5 embryos and 590 trajectories for Control Mo, n=7 embryos and 753 trajectories for Bra Mo, n=5 Embryos and 874 trajectories for Sox2 Mo). Scale bar is 100 µm.

Figure 6: Spatial heterogeneity and gradient models. A: Initial condition of the gradient model. Close up of the progenitor region showing the spatial organization of Sox2/Bra levels in gradient (bottom panel). **B**: Evolution of cell numbers for each cell type for the gradient model. **C**: Tissue cell motilities in the gradient model. **D** Evolution of the gradient model through different time points 0, 5hrs and 10 hrs. **E**: Comparison of the gradient and heterogeneous simulation at 10hrs with elongation rates. **F**.Y displacement of resident progenitors chosen at the center of the PZ for both models. Value below the graphs are averages. **G:** Initial (left) and final (right) shapes of the progenitor region of the heterogeneous (yellow) and the gradient model (pink). Conservation or proportions are noted in percentage. **H**: MSD for progenitors in both models.

Supplemental Figure 1: Co-expression and heterogeneity of expression of Sox2 and Bra protein starts around stage HH5 in quail embryos. A: Sox2 and Bra average expression in the progenitor region at different stages of development. Sox2 and Bra expression at the embryo (**B-D**) and cellular levels in the progenitor zone (**E-F**). Stage HH4 (**B,E**); Stage HH5 (**C,F**), Stage HH6 (**D,G**). Note that co-expression of Sox2 and Bra as well as cell-to-cell heterogeneity start to be detectable from stage 5HH onward.

Supplemental Figure 2: Chicken NMPs co express Sox2 and Bra protein with a high degree of cell-to-cell heterogeneity. Sox2 and Bra protein expression in the progenitor region of stage HH10 chicken embryo. Ventral view of the posterior part of the embryo (**A-D**). Close up imaging within the progenitor region (dashes white square in **D**) (**E-H**). Image corresponding to the DAPI signal (**A-E**), Bra signal (**B,F**), Sox2 signal (**C,D**), merged of Dapi, Bra, Sox2 signals. Note the variability in Sox and Bra expression in chicken progenitor visible in **D** and **H**.

<u>Supplemental Figure 3</u>: Sox2 and Bra tissue expression in opposite gradient at the tissue level of the progenitor zone of stage 10-11HH of quail embryo

A: Sox2 (green) and Bra (red) expression has been analyzed at the tissue scale in the caudal part of stage HH11 quail embryo, in the progenitor region (dashed white rectangle). **B**: Chart displaying the Sox2 and Bra levels at different antero/posterior and dorso ventral levels (n= 9 embryos, thick lines are the averages, thin lines demarcated the SEM).

<u>Supplemental Figure 4</u>: Efficiency of Sox2 and Bra upregulation and downregulation experiments.

Effect of Pcig-Sox2 (**A-C**), Sox2-Mo (**D-E**), Pcig-Bra (**G-I**) ,and Bra-Mo (**J-L**), 7 hours after electroporation in the PZ. GFP signal (**A,D,G,J**) , Sox2 signal (**B,E**), Bra signal (**H-K**), and merge images (**C,F,I,L**). Note that in the case of overexpression the localization of the GFP corresponds to an elevated expression of the targeted protein (yellow arrows) whereas in the case of Mo it corresponds to a lower level of the protein in comparison (blue arrows) to neighboring non-transfected cells.

<u>Supplemental Figure 5</u>: Quantification of Sox2 and Bra protein expression levels during upregulation and downregulation experiments. A: Analysis of Bra levels in Pcig-Bra versus Pcig overexpressing cells, Bra electroporation leads to significant upregulation of Bra. **B**: Analysis of Sox2 levels in Pcig-Sox2 versus Pcig overexpressing cells; Sox2 electroporation leads to significant upregulation of Sox2 . **C**: Analysis of Bra levels in Pcig-Sox2 versus Pcig overexpressing cells, Sox2 electroporation leads to significant downregulation of Bra. **D**: Analysis of Sox2 levels in Pcig-Bra versus Pcig overexpressing cells, Bra electroporation leads to significant down regulation of Sox2. **E**: Analysis of Bra levels in Mo-Bra versus control Mo electroporated cells, Bra-Mo electroporation leads to significant downregulation of Bra. **F**: Analysis of Sox2 levels in Sox2-Mo versus control Mo electroporated cells, Sox2-Mo electroporation leads to significant downregulation of Sox2. **G**: Analysis of Bra levels in Sox2-Mo versus control Mo electroporated cells, Sox2-Mo electroporation leads to significant upregulation of Bra. **H**: Analysis of Sox2 levels in Bra-Mo versus control Mo overexpressing cells. Bra-Mo electroporation does not lead to significant changes in Sox2 expression levels. Levels of expression are normalized to non-electroporated cells of the same sample.

Supplemental Figure 6: Distribution of motility frequencies within the progenitor region the paraxial mesoderm and the neural tube. Representation of the distribution of frequency for different classes of speeds ranging from slow moving cells to fast moving cells corresponding to figure 3C corrected motility. Top panel correspond to the progenitor zone, middle panel to the PSM and bottom panel to the neural tube. Note that the distributions of speed are different between the three groups, the neural tube having more slow cells than the two other tissues and the progenitor zone having slightly more slower than the PSM (higher histogram pointed by the blue arrow).

<u>Supplemental Figure 7</u>: Effect of Sox2 and Bra on raw cell and tissue movements. Elongation (**A,C**), raw cell movements (**B,D**) and raw angle distribution (**E,F**) measurements for Sox2 And Bra overexpression (**A,B,E**) and down regulation (**C,D,F**).

<u>Supplemental Figure 8:</u> Analysis of directionality in the gradient model.

Distribution of directionalities of migration within the progenitor zone (PZ), PSM and neural tube (NT) of the gradient model.

Supplemental Movie 1: Progenitor migration in control condition (corresponding to Figure 3). H2B-GFP electroporated quail embryos. The movie show a ventral view of the posterior region of a representative embryo (10X). GFP signal is in green, bright field in blue. Moving regions of interest are delineated as follow: yellow for the progenitor, red for the nascent paraxial mesoderm and green for the neural tube. Cellular trajectories are marked and colored accordingly

Supplemental Movie 2: Mathematical simulation of posterior region behavior. Heterogeneous expression of Sox2 and Bra.

Supplemental Movie 3: Mathematical simulation of posterior region behavior. Heterogeneous expression of Sox2 and Bra, initial ratios are set up for 50%.

Supplemental Movie 4: Mathematical simulation of posterior progenitors behavior. Heterogeneous expression of Sox2 and Bra, Low Sox2/Bra (high Bra)

Supplemental Movie 5: Mathematical simulation of posterior progenitors behavior. Spatially heterogeneous expression of Sox2 and Bra, High Sox2/Bra (high Sox2)

Supplemental Movie 6: Progenitor migration in Sox2 and Bra overexpression experiments (Corresponding to Figure 5). The movie show ventral views of posterior regions of three representative embryos, focused on the PZ (set as a reference point), which has been set as a reference point (10X). GFP signal is in green, bright field in blue. Cellular trajectories are marked and colored in yellow. Bra overexpression is on the left, Sox2 overexpression on the right. Control embryo in the middle.

Supplemental Movie 7: Progenitor migration in Sox2 and Bra Mo experiments (Corresponding to Figure 5). The movie show ventral views of posterior regions of three representative embryos, focused on the PZ (set as a reference point), which has been set as a reference point (10X). GFP signal is in green, bright field in blue. Cellular trajectories are marked and colored in yellow. Bra Mo is on the left, Sox2 Mo on the right. Control embryo in the middle.

Supplemental Movie 8: Mathematical simulation of posterior progenitor's behavior. Graded expression of Sox2 and Bra.

Supplemental Movie 9: Comparison of gradient (left) and heterogeneous model (right).

Bibliography

1. Farrell JA, Wang Y, Riesenfeld SJ, Shekhar K, Regev A, Schier AF. Single-cell reconstruction of developmental trajectories during zebrafish embryogenesis. Science. 2018 Jun 1;360(6392).

2. Wagner DE, Weinreb C, Collins ZM, Briggs JA, Megason SG, Klein AM. Single-cell mapping of gene expression landscapes and lineage in the zebrafish embryo. Science. 2018 Jun 1;360(6392):981–987.

3. Selleck MA, Stern CD. Fate mapping and cell lineage analysis of Hensen's node in the chick embryo. Development. 1991 Jun;112(2):615–626.

4. Iimura T, Yang X, Weijer CJ, Pourquié O. Dual mode of paraxial mesoderm formation during chick gastrulation. Proc Natl Acad Sci USA. 2007 Feb 20;104(8):2744–2749.

5. Wilson V, Beddington RS. Cell fate and morphogenetic movement in the late mouse primitive streak. Mech Dev. 1996 Mar;55(1):79–89.

6. Psychoyos D, Stern CD. Fates and migratory routes of primitive streak cells in the chick embryo. Development. 1996 May;122(5):1523–1534.

7. Cambray N, Wilson V. Axial progenitors with extensive potency are localised to the mouse chordoneural hinge. Development. 2002 Oct;129(20):4855–4866.

8. McGrew MJ, Sherman A, Lillico SG, Ellard FM, Radcliffe PA, Gilhooley HJ, et al. Localised axial progenitor cell populations in the avian tail bud are not committed to a posterior Hox identity. Development. 2008 Jul;135(13):2289–2299.

9. Tzouanacou E, Wegener A, Wymeersch FJ, Wilson V, Nicolas J-F. Redefining the progression of lineage segregations during mammalian embryogenesis by clonal analysis. Dev Cell. 2009 Sep;17(3):365–376.

10. Attardi A, Fulton T, Florescu M, Shah G, Muresan L, Lenz MO, et al. Neuromesodermal progenitors are a conserved source of spinal cord with divergent growth dynamics. Development. 2018 Nov 9;145(21).

11. Griffith CM, Wiley MJ, Sanders EJ. The vertebrate tail bud: three germ layers from one tissue. Anat Embryol (Berl). 1992;185(2):101–113.

12. Herrmann BG, Labeit S, Poustka A, King TR, Lehrach H. Cloning of the T gene required in mesoderm formation in the mouse. Nature. 1990 Feb 15;343(6259):617–622.

13. Bergsland M, Ramsköld D, Zaouter C, Klum S, Sandberg R, Muhr J. Sequentially acting Sox transcription factors in neural lineage development. Genes Dev. 2011 Dec 1;25(23):2453–2464.

14. Takemoto T, Uchikawa M, Yoshida M, Bell DM, Lovell-Badge R, Papaioannou VE, et al. Tbx6-dependent Sox2 regulation determines neural or mesodermal fate in axial stem cells. Nature. 2011 Feb 17;470(7334):394–398.

15. Wilson V, Manson L, Skarnes WC, Beddington RS. The T gene is necessary for normal mesodermal morphogenetic cell movements during gastrulation. Development. 1995 Mar;121(3):877–886.

16. Wilson V, Beddington R. Expression of T protein in the primitive streak is necessary and sufficient for posterior mesoderm movement and somite differentiation. Dev Biol. 1997 Dec 1;192(1):45–58.

17. Olivera-Martinez I, Harada H, Halley PA, Storey KG. Loss of FGF-dependent mesoderm identity and rise of endogenous retinoid signalling determine cessation of body axis elongation. PLoS Biol. 2012 Oct 30;10(10):e1001415.

18. Wymeersch FJ, Huang Y, Blin G, Cambray N, Wilkie R, Wong FCK, et al. Position-dependent plasticity of distinct progenitor types in the primitive streak. Elife. 2016 Jan 18;5:e10042.

19. Koch F, Scholze M, Wittler L, Schifferl D, Sudheer S, Grote P, et al. Antagonistic Activities of Sox2 and Brachyury Control the Fate Choice of Neuro-Mesodermal Progenitors. Dev Cell. 2017 Sep 11;42(5):514–526.e7.

20. Bénazéraf B, Francois P, Baker RE, Denans N, Little CD, Pourquié O. A random cell motility gradient downstream of FGF controls elongation of an amniote embryo. Nature. 2010 Jul 8;466(7303):248–252.

21. Bénazéraf B, Beaupeux M, Tchernookov M, Wallingford A, Salisbury T, Shirtz A, et al. Multi-scale quantification of tissue behavior during amniote embryo axis elongation. Development. 2017 Dec 1;144(23):4462–4472.

22. Kawachi T, Shimokita E, Kudo R, Tadokoro R, Takahashi Y. Neural-fated self-renewing cells regulated by Sox2 during secondary neurulation in chicken tail bud. Dev Biol. 2020 May 15;461(2):160–171.

23. Goto H, Kimmey SC, Row RH, Matus DQ, Martin BL. FGF and canonical Wnt signaling cooperate to induce paraxial mesoderm from tailbud neuromesodermal progenitors through regulation of a two-step epithelial to mesenchymal transition. Development. 2017 Apr 15;144(8):1412–1424.

24. Ciruna B, Rossant J. FGF signaling regulates mesoderm cell fate specification and morphogenetic movement at the primitive streak. Dev Cell. 2001 Jul;1(1):37–49.

25. Yamaguchi TP, Takada S, Yoshikawa Y, Wu N, McMahon AP. T (Brachyury) is a direct target of Wnt3a during paraxial mesoderm specification. Genes Dev. 1999 Dec 15;13(24):3185–3190.

26. Garriock RJ, Chalamalasetty RB, Kennedy MW, Canizales LC, Lewandoski M, Yamaguchi TP. Lineage tracing of neuromesodermal progenitors reveals novel Wnt-dependent roles in trunk progenitor cell maintenance and differentiation. Development. 2015 May 1;142(9):1628–1638.

27. Bouldin CM, Manning AJ, Peng Y-H, Farr GH, Hung KL, Dong A, et al. Wnt signaling and tbx16 form a bistable switch to commit bipotential progenitors to mesoderm. Development. 2015 Jul 15;142(14):2499–2507.

28. Gouti M, Delile J, Stamataki D, Wymeersch FJ, Huang Y, Kleinjung J, et al. A Gene Regulatory Network Balances Neural and Mesoderm Specification during Vertebrate Trunk Development. Dev Cell. 2017 May 8;41(3):243–261.e7.

29. Cunningham TJ, Colas A, Duester G. Early molecular events during retinoic acid induced differentiation of neuromesodermal progenitors. Biol Open. 2016 Dec 15;5(12):1821–1833.

30. Mathis L, Kulesa PM, Fraser SE. FGF receptor signalling is required to maintain neural progenitors during Hensen's node progression. Nat Cell Biol. 2001 Jun;3(6):559–566.

31. Dias A, Lozovska A, Wymeersch FJ, Nóvoa A, Binagui-Casas A, Sobral D, et al. A Tgfbr1/Snai1-dependent developmental module at the core of vertebrate axial elongation. Elife. 2020 Jun 29;9.

32. Xiong F, Ma W, Bénazéraf B, Mahadevan L, Pourquié O. Mechanical Coupling Coordinates the Co-elongation of Axial and Paraxial Tissues in Avian Embryos. Dev Cell. 2020 Sep 5;

33. Roszko I, Faure P, Mathis L. Stem cell growth becomes predominant while neural plate progenitor pool decreases during spinal cord elongation. Dev Biol. 2007 Apr 1;304(1):232–245.

34. Hashimoto K, Fujimoto H, Nakatsuji N. An ECM substratum allows mouse mesodermal cells isolated from the primitive streak to exhibit motility similar to that inside the embryo and reveals a deficiency in the T/T mutant cells. Development. 1987 Aug;100(4):587–598.

35. Lawton AK, Nandi A, Stulberg MJ, Dray N, Sneddon MW, Pontius W, et al. Regulated tissue fluidity steers zebrafish body elongation. Development. 2013 Feb 1;140(3):573–582.

36. Mongera A, Rowghanian P, Gustafson HJ, Shelton E, Kealhofer DA, Carn EK, et al. A fluid-to-solid jamming transition underlies vertebrate body axis elongation. Nature. 2018 Sep 5;561(7723):401–405.

37. Joubin K, Stern CD. Molecular interactions continuously define the organizer during the cell movements of gastrulation. Cell. 1999 Sep 3;98(5):559–571.

38. Yuan S, Schoenwolf GC. Reconstitution of the organizer is both sufficient and required to re-establish a fully patterned body plan in avian embryos. Development. 1999 Jun 1;126(11):2461–2473.

39. Prasetyanti PR, Medema JP. Intra-tumor heterogeneity from a cancer stem cell perspective. Mol Cancer. 2017 Feb 16;16(1):41.

40. Ainsworth SJ, Stanley RL, Evans DJR. Developmental stages of the Japanese quail. J Anat. 2010 Jan;216(1):3–15.

41. Hamburger V, Hamilton HL. A series of normal stages in the development of the chick embryo. J Morphol. 1951 Jan;88(1):49–92.

42. Chapman SC, Collignon J, Schoenwolf GC, Lumsden A. Improved method for chick whole-embryo culture using a filter paper carrier. Dev Dyn. 2001 Mar;220(3):284–289.

43. Megason SG, McMahon AP. A mitogen gradient of dorsal midline Wnts organizes growth in the CNS. Development. 2002 May;129(9):2087–2098.

44. Roellig D, Tan-Cabugao J, Esaian S, Bronner ME. Dynamic transcriptional signature and cell fate analysis reveals plasticity of individual neural plate border cells. Elife. 2017 Mar 29;6.

45. Iimura T, Pourquié O. Manipulation and electroporation of the avian segmental plate and somites in vitro. Methods Cell Biol. 2008;87:257–270.

46. Thévenaz P, Ruttimann UE, Unser M. A pyramid approach to subpixel registration based on intensity. IEEE Trans Image Process. 1998;7(1):27–41.

47. Sbalzarini IF, Koumoutsakos P. Feature point tracking and trajectory analysis for video imaging in cell biology. J Struct Biol. 2005 Aug;151(2):182–195.

48. Guillot C, Michaut A, Rabe B, Pourquié O Dynamics of primitive streak regression controls the fate of neuro-mesodermal progenitors in the chicken embryo https://doi.org/10.1101/2020.05.04.077586.

49. Elena Gonzalez-Gobartt, José Blanco-Ameijeiras, Susana Usieto, Guillaume Allio, Bertrand Benazeraf, Elisa Martí. Cell intercalation driven by SMAD3 underlies secondary neural tube formation. https://doi.org/10.1101/2020.08.24.261008

50. Timothy R. Wood, Anders Kyrsting, Johannes Stegmaier, Iwo Kucinski, Clemens F. Kaminski, Ralf Mikut, Octavian Voiculescu. Neuromesodermal progenitors separate the axial stem zones while producing few single- and dual-fated descendants. https://doi.org/10.1101/622571

51. Tatiana Solovieva, Hui-Chun Lu, Adam Moverley, Nicolas Plachta, Claudio D. Stern The embryonic node functions as an instructive stem cell niche. https://doi.org/10.1101/2020.11.10.376913

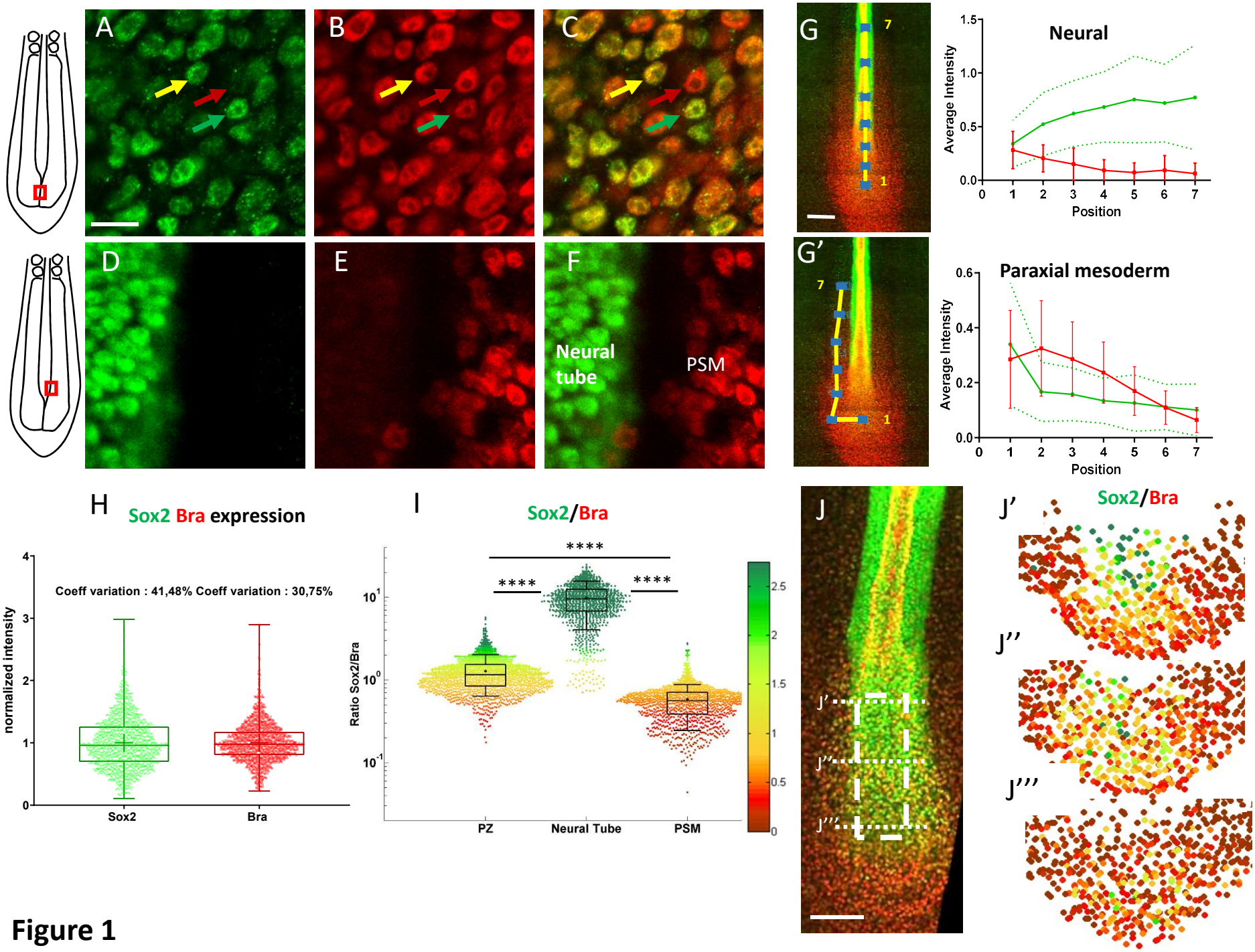
A
B
C
D
E
F
Neural tube
PSM
G
G'
7
1
Neural
Average Intensity
Position
Paraxial mesoderm
H
Sox2 Bra expression
Coeff variation : 41,48% Coeff variation : 30,75%
normalized intensity
Sox2
Bra
I
Sox2/Bra
****
Ratio Sox2/Bra
PZ
Neural Tube
PSM
J
J'
J''
J'''
Sox2/Bra

Figure 1

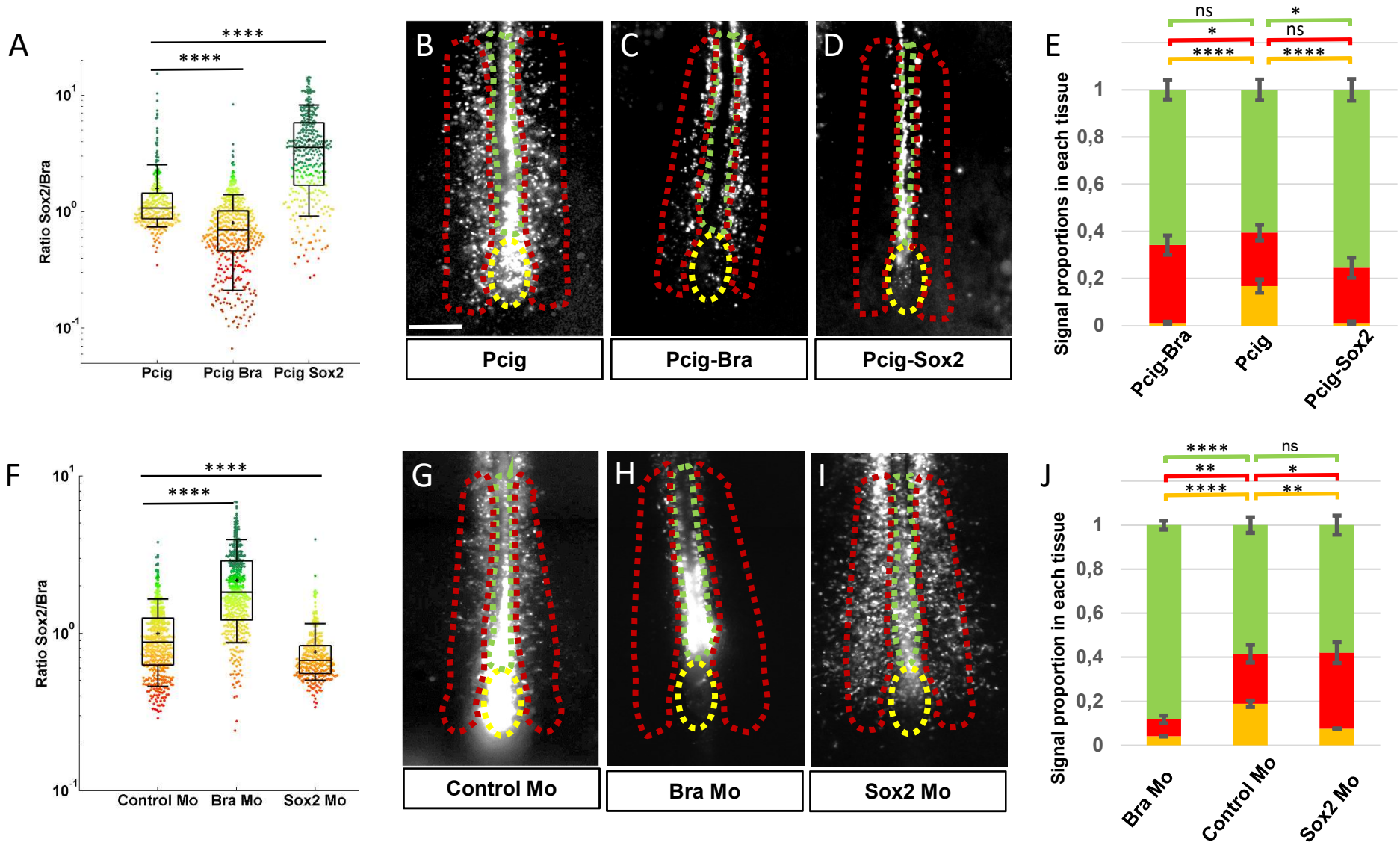
A
****
****
Ratio Sox2/Bra
Pcig
Pcig Bra
Pcig Sox2
B
C
D
Pcig
Pcig-Bra
Pcig-Sox2
E
ns
*
ns
*
****
****
Signal proportions in each tissue
Pcig-Bra
Pcig
Pcig-Sox2
F
****
****
Ratio Sox2/Bra
Control Mo
Bra Mo
Sox2 Mo
G
H
I
Control Mo
Bra Mo
Sox2 Mo
J
****
ns
**
*
****
**
Signal proportion in each tissue
Bra Mo
Control Mo
Sox2 Mo

Figure 2

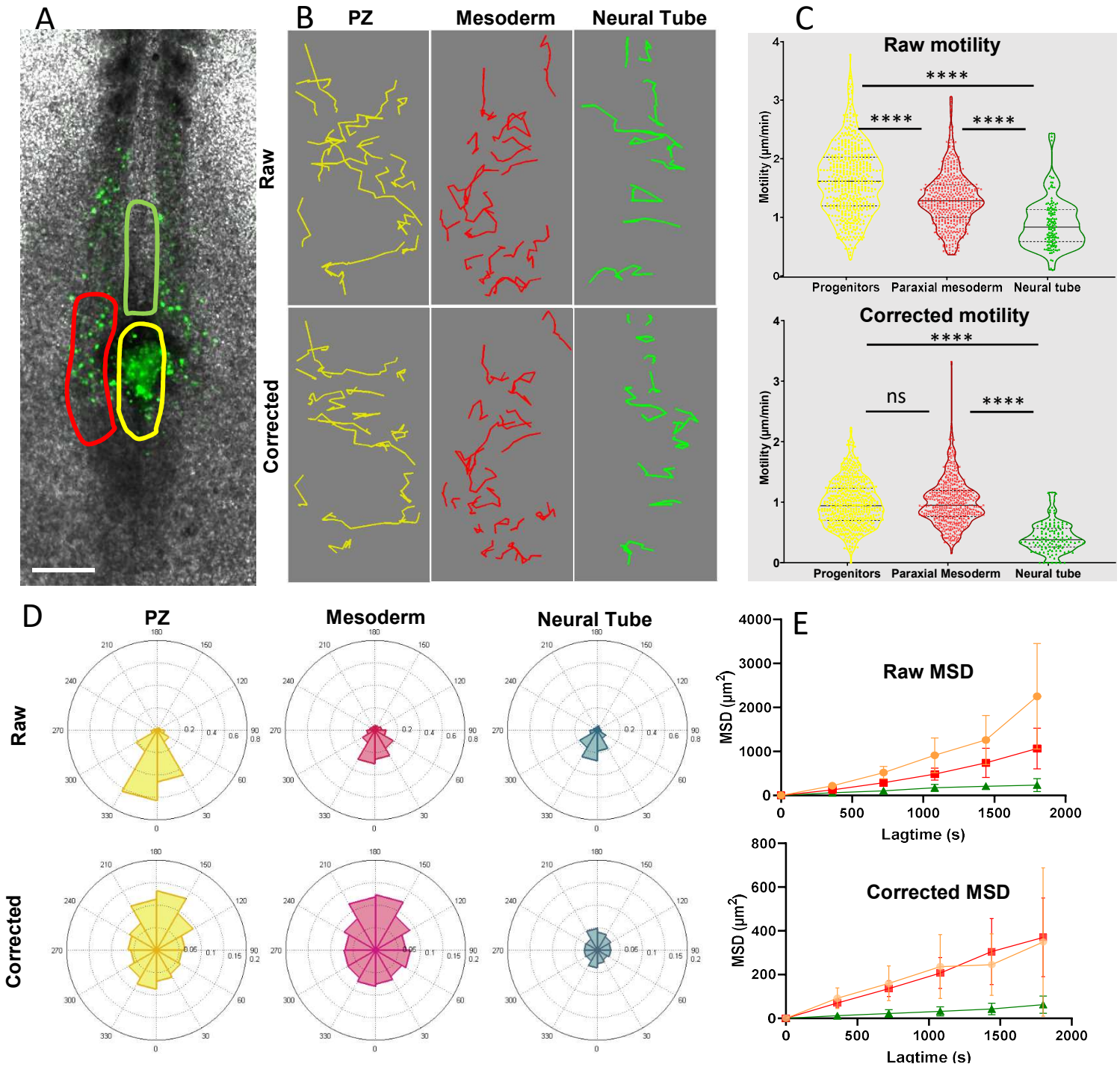
A
B
PZ
Mesoderm
Neural Tube
Raw
Corrected
C
Raw motility
****
****
****
Motility (µm/min)
Progenitors
Paraxial mesoderm
Neural tube
Corrected motility
****
ns
****
Motility (µm/min)
Progenitors
Paraxial Mesoderm
Neural tube
D
PZ
Mesoderm
Neural Tube
Raw
Corrected
E
Raw MSD
MSD (µm²)
Lagtime (s)
Corrected MSD
MSD (µm²)
Lagtime (s)

Figure 3

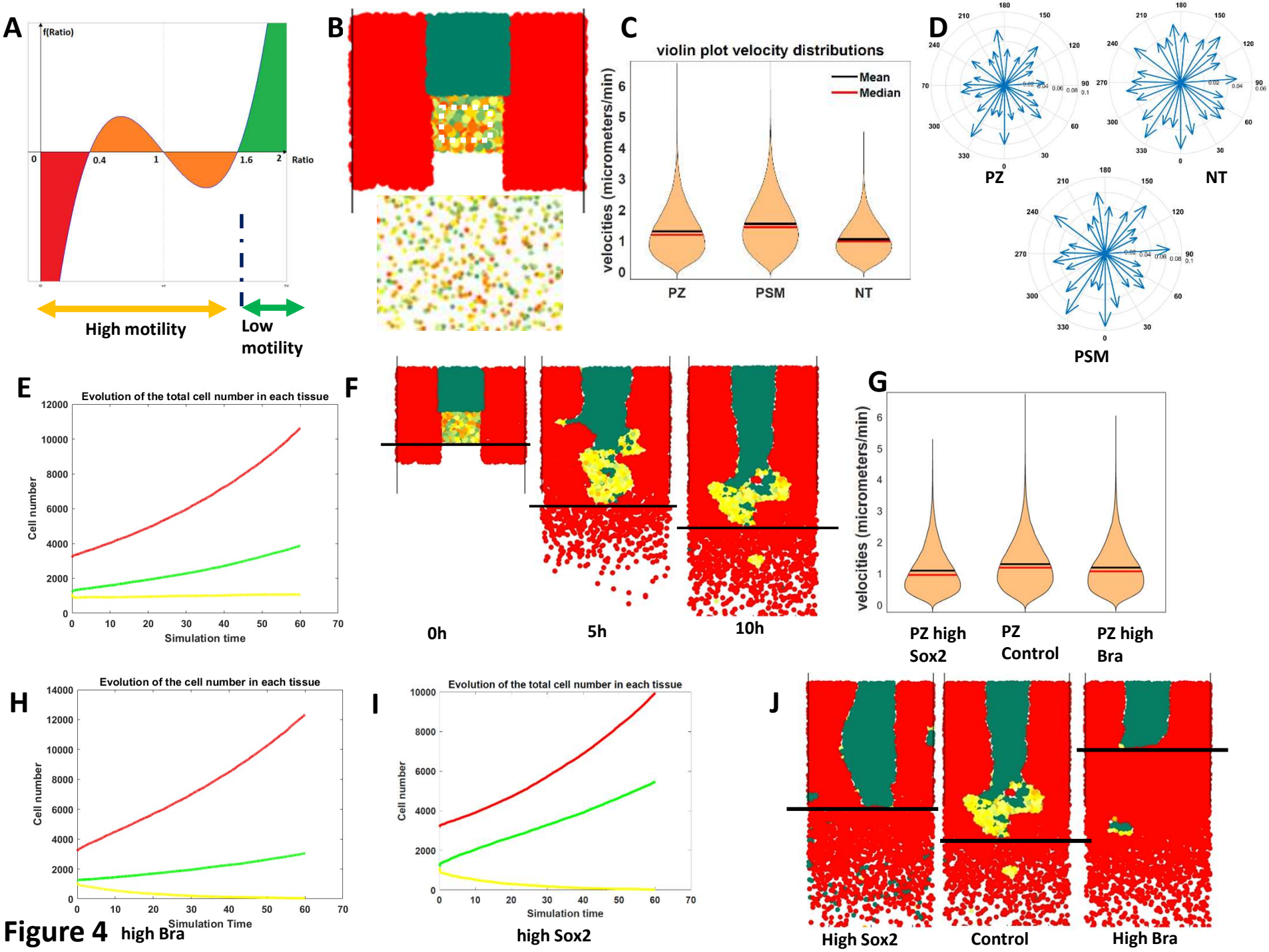
A
f(Ratio)
0
0.4
1
1.6
2
Ratio
High motility
Low motility
B
C
violin plot velocity distributions
Mean
Median
velocities (micrometers/min)
PZ
PSM
NT
D
PZ
NT
PSM
E
Evolution of the total cell number in each tissue
Cell number
Simulation time
F
0h
5h
10h
G
velocities (micrometers/min)
PZ high Sox2
PZ Control
PZ high Bra
H
Evolution of the cell number in each tissue
Cell number
Simulation Time
high Bra
I
Evolution of the total cell number in each tissue
Cell number
Simulation time
high Sox2
J
High Sox2
Control
High Bra

Figure 4

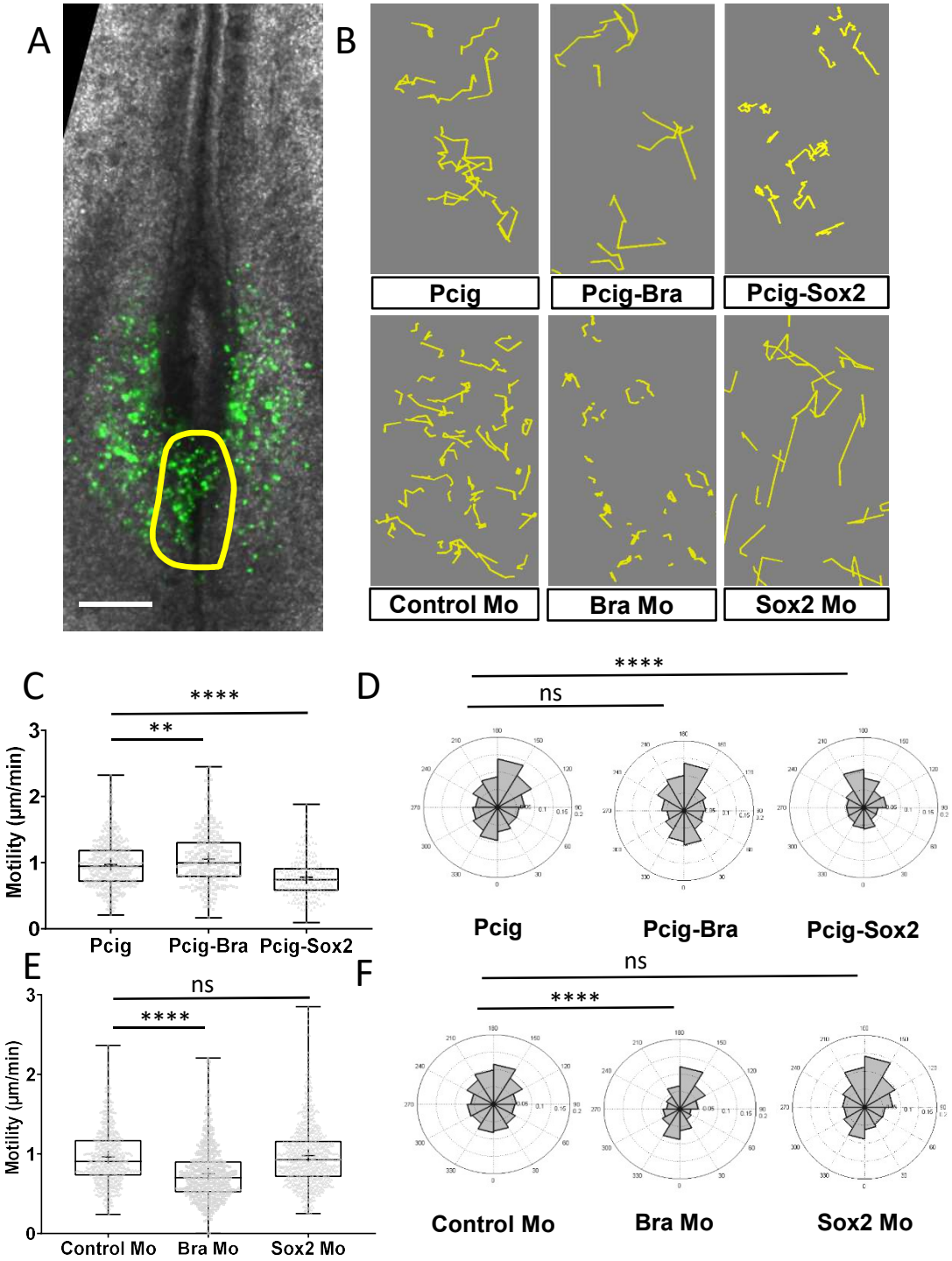
A
B
Pcig
Pcig-Bra
Pcig-Sox2
Control Mo
Bra Mo
Sox2 Mo
C
****
**
Motility (µm/min)
Pcig
Pcig-Bra
Pcig-Sox2
D
****
ns
Pcig
Pcig-Bra
Pcig-Sox2
E
ns
****
Motility (µm/min)
Control Mo
Bra Mo
Sox2 Mo
F
ns
****
Control Mo
Bra Mo
Sox2 Mo

Figure 5

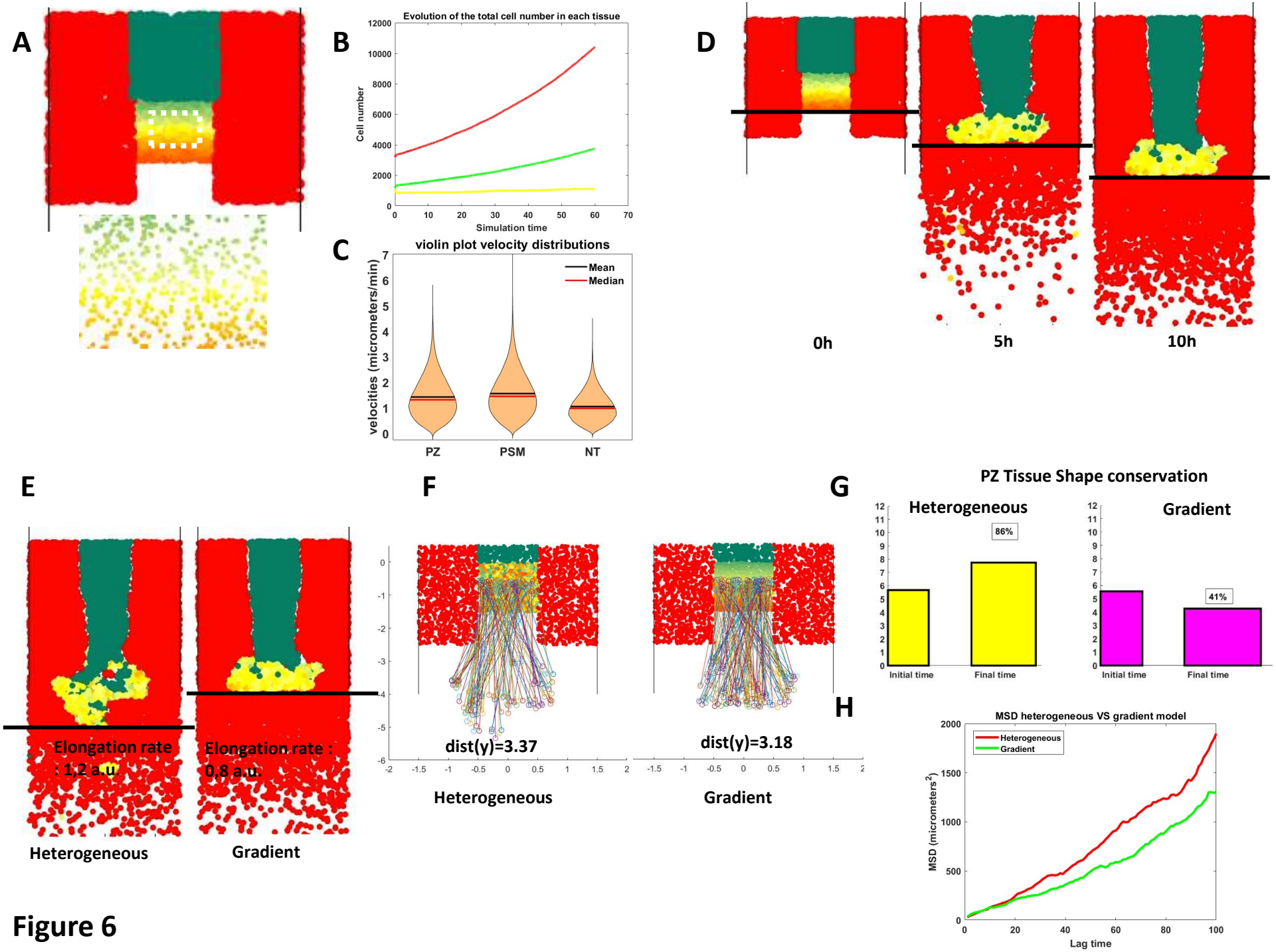
A
B
Evolution of the total cell number in each tissue
Cell number
Simulation time
C
violin plot velocity distributions
velocities (micrometers/min)
Mean
Median
PZ
PSM
NT
D
0h
5h
10h
E
Elongation rate : 1,2 a.u.
Elongation rate : 0,8 a.u.
Heterogeneous
Gradient
F
dist(y)=3.37
dist(y)=3.18
Heterogeneous
Gradient
G
PZ Tissue Shape conservation
Heterogeneous
Gradient
86%
41%
Initial time
Final time
H
MSD heterogeneous VS gradient model
Heterogeneous
Gradient
MSD (micrometers^2)
Lag time

Figure 6

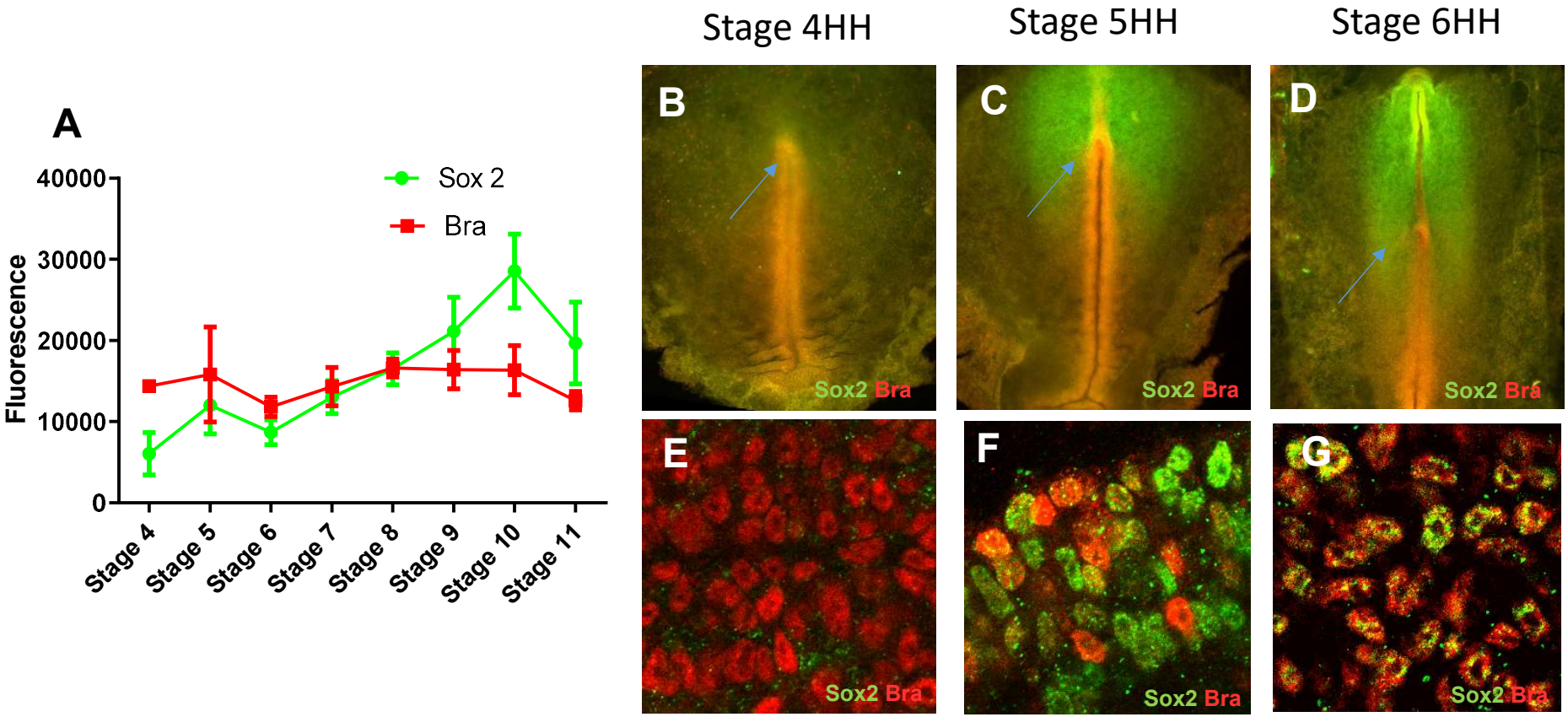

Supplemental Figure 1

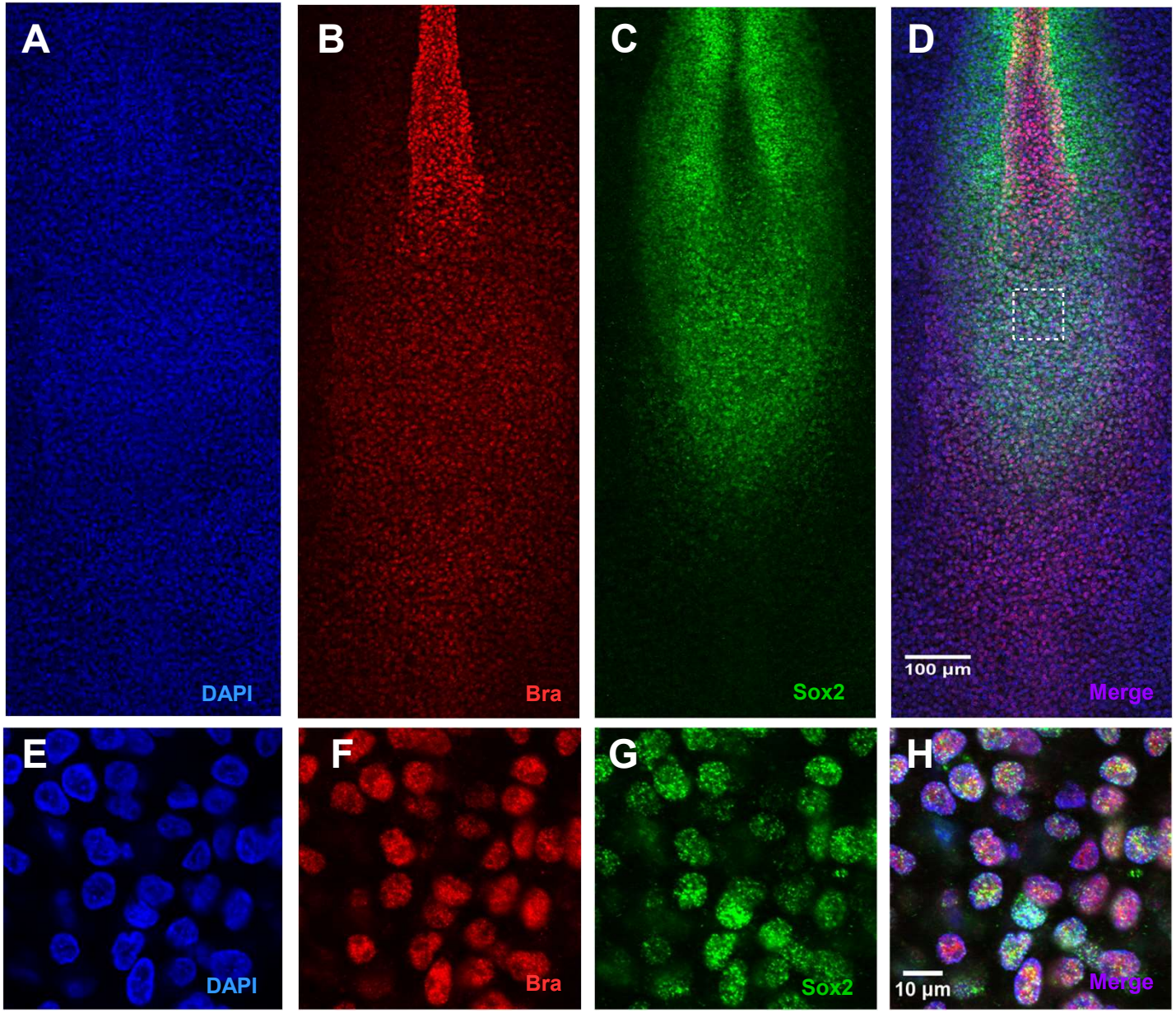

Supplemental Figure 2

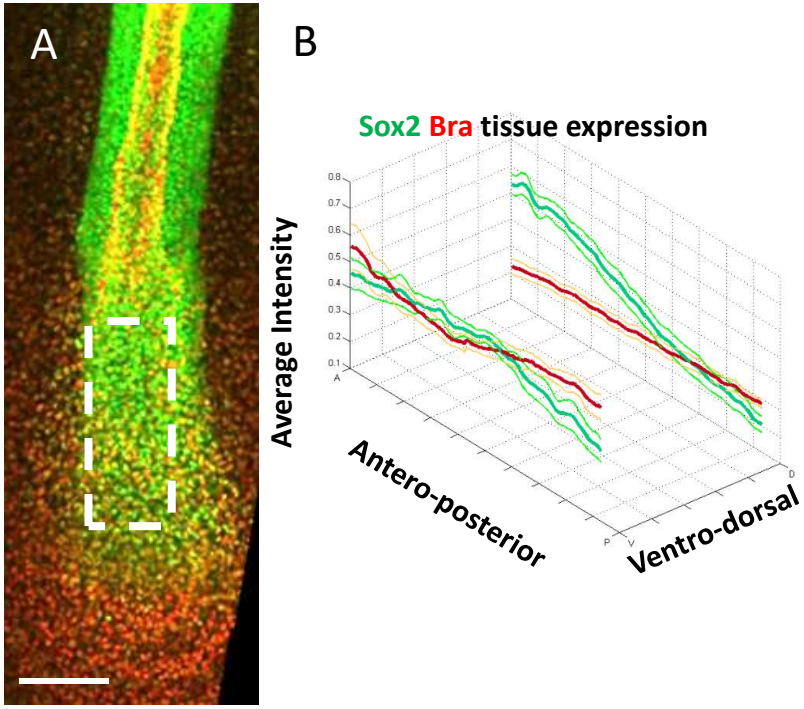

Supplemental Figure 3

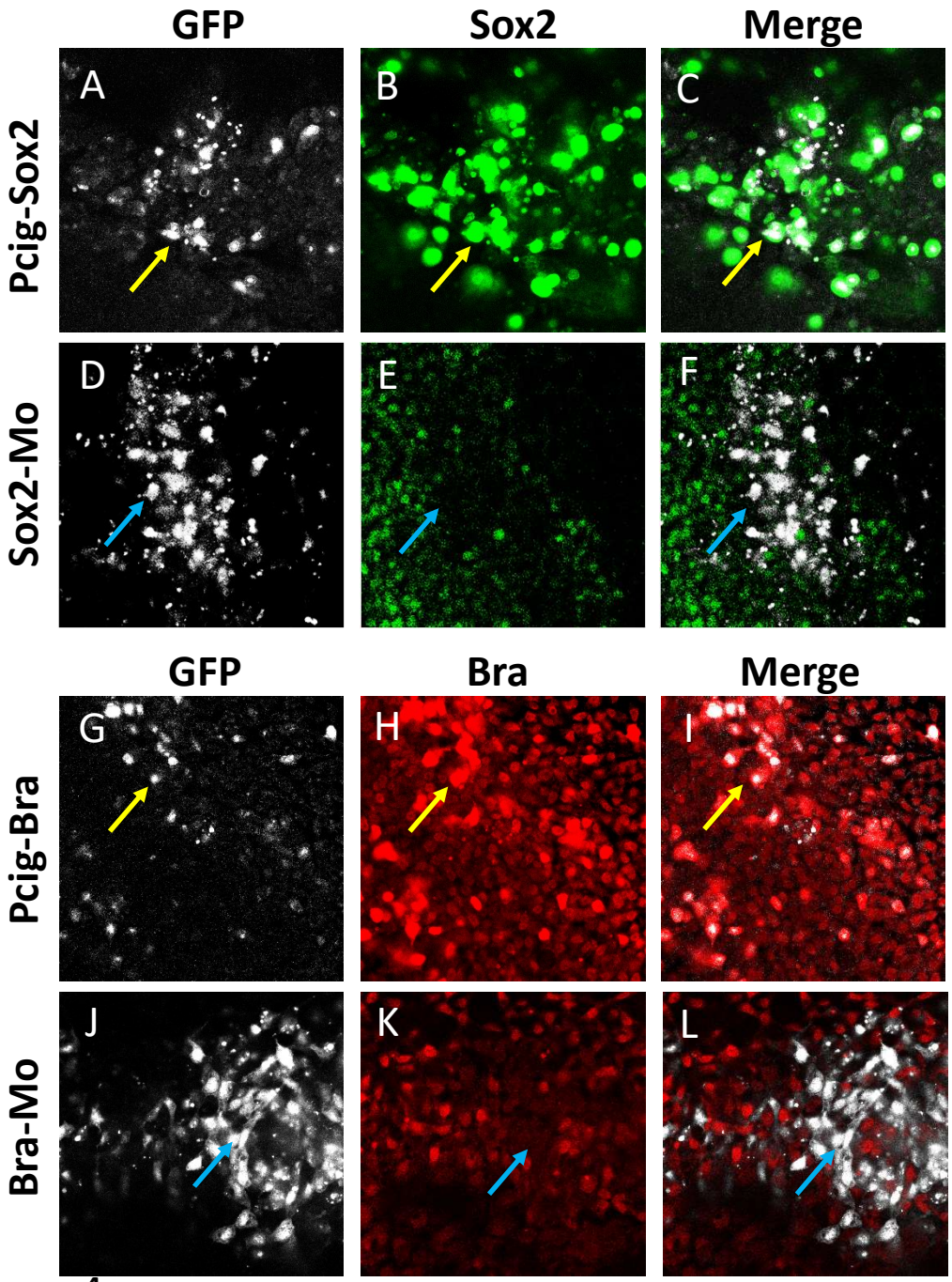

Supplemental Figure 4

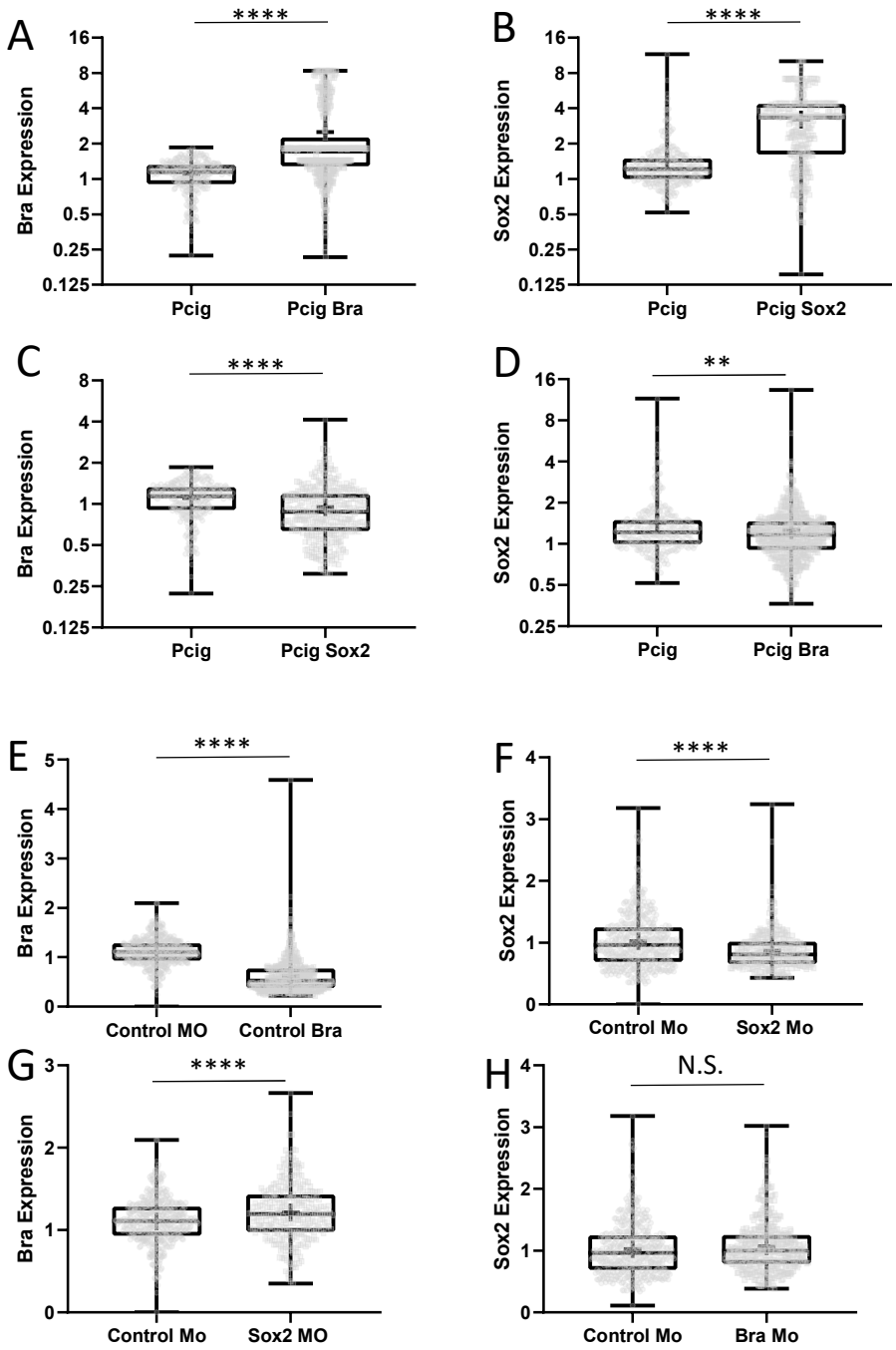

Supplemental Figure 5

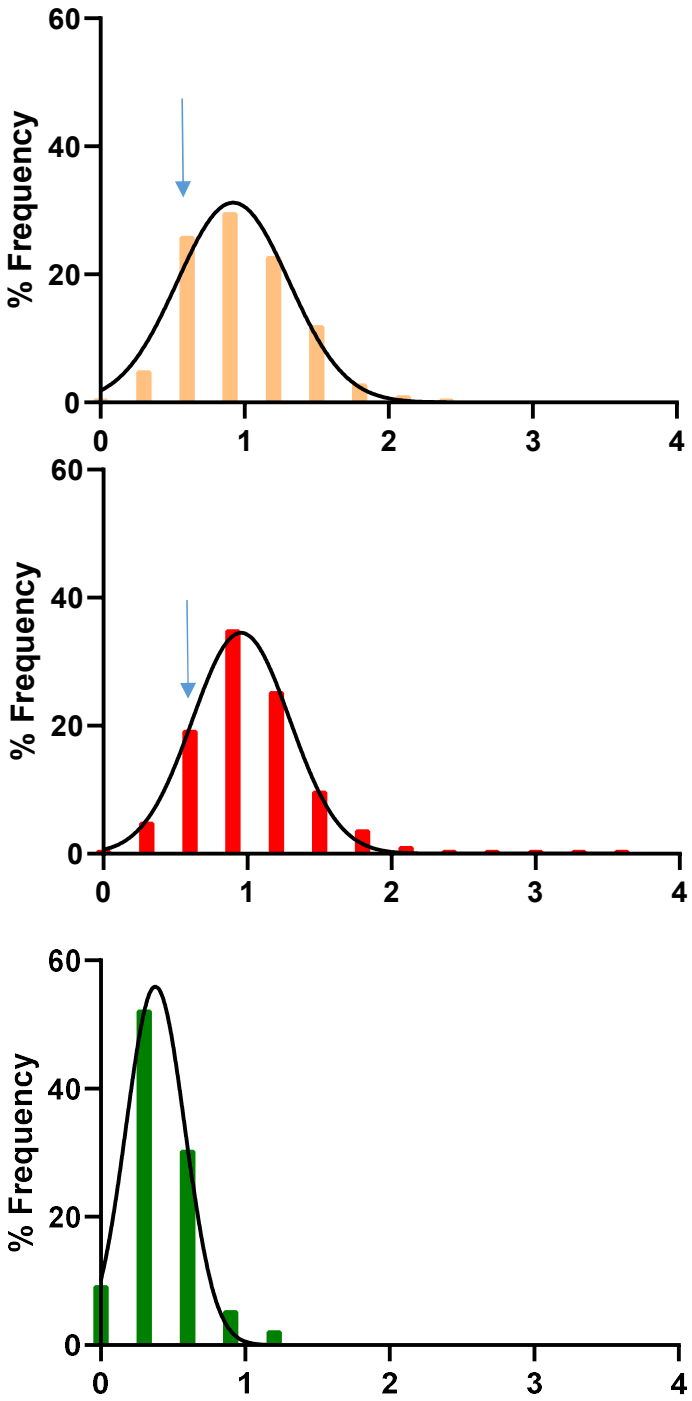

Supplemental Figure 6

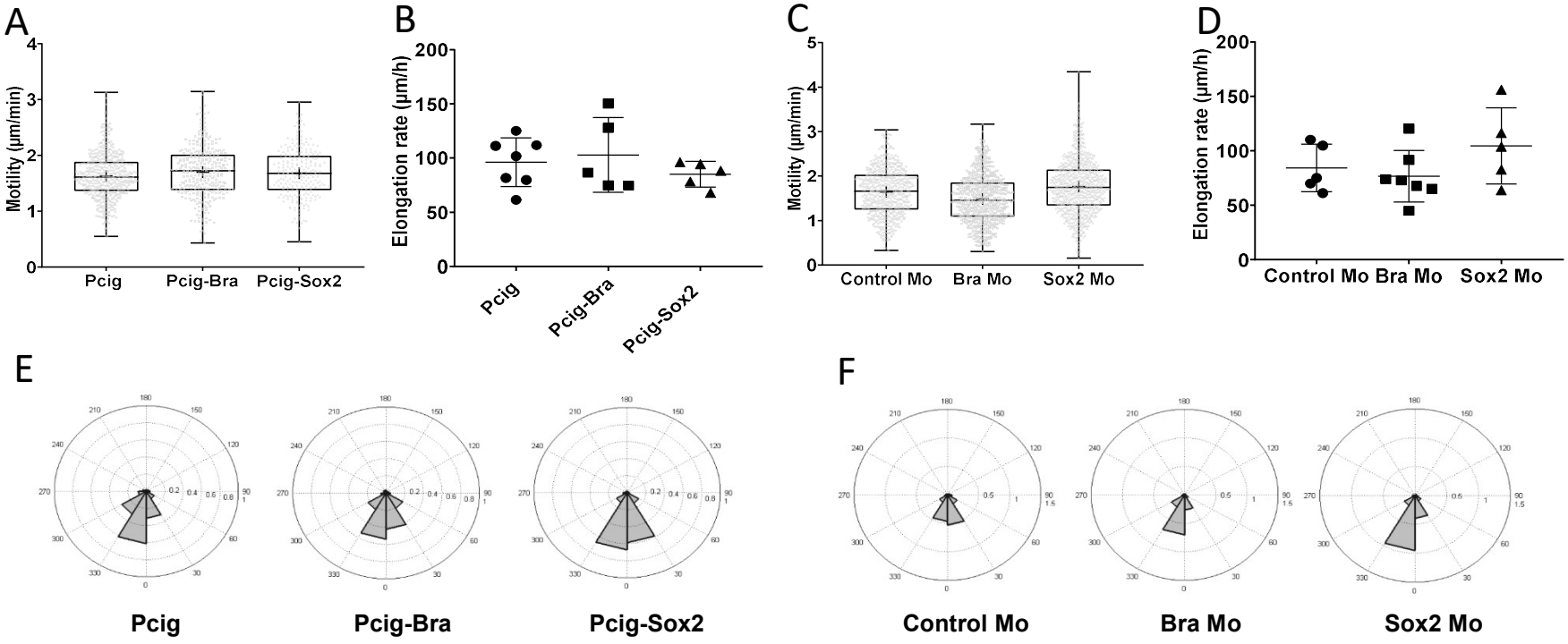

Supplemental Figure 7

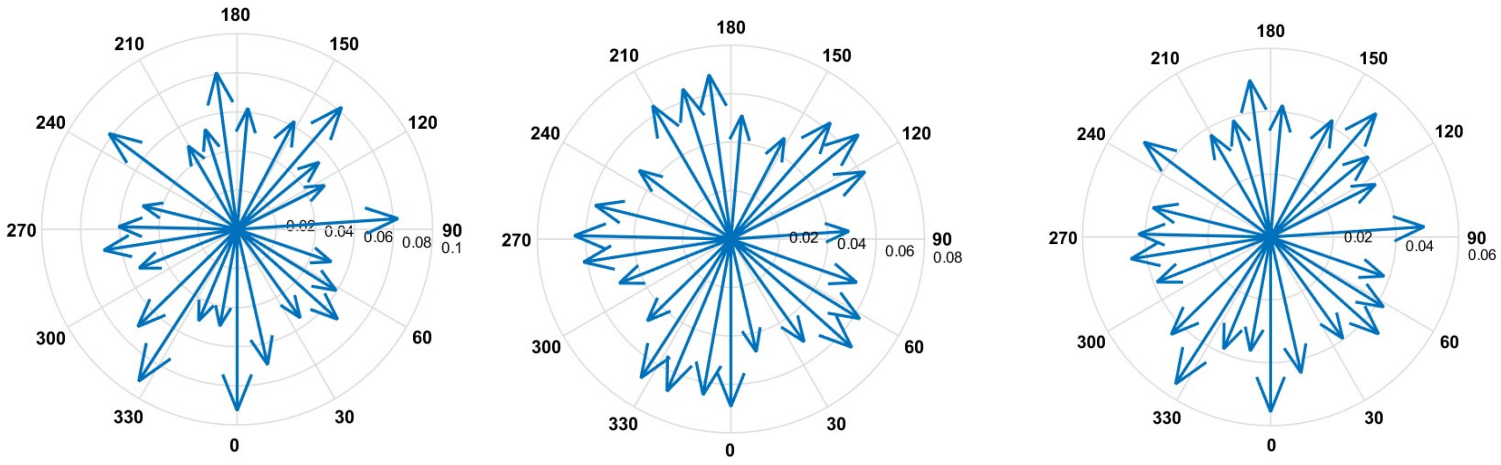

PSM gradient **PZ gradient** **NT gradient**

Supplemental Figure 8